THE ULTRASONOGRAPHIC MEASUREMENT OF MUSCLE ARCHITECTURE

THE EFFECT OF ULTRASOUND PROBE ORIENTATION ON THE MEASUREMENT OF MUSCLE ARCHITECTURE PARAMETERS.

by

Marc Klimstra, B.Kin., B.Ed.

A THESIS

Submitted to the School of Graduate Studies

In Partial Fulfillment of the Requirements

For the Degree

Master of Science

McMaster University

MASTER OF SCIENCE (2004)
(Human Biodynamics)

McMaster University
Hamilton, Ontario

Title: The Effect of Ultrasound Probe Orientation on the Measurement of Muscle Architecture Parameters.

Author: Marc Klimstra, B. Ed. (University of Western Ontario)
B. Kin. (McMaster University)

Supervisor: Dr. James J. Dowling, Ph. D.

Number of Pages: ix, 96

Abstract

A slow concentric contraction of the tibialis anterior muscle was imaged using Brightness-Mode Ultrasonography (BMU) from different probe orientations to determine the effect of probe orientation on the measurement of muscle architecture parameters (MAP). Nine contractions were performed by each of nine subjects. Each contraction was visualized with a different probe orientation on the anterior surface of the muscle. Data was taken from the same four joint angles from all contractions from all subjects and then compared for values of torque, tibialis anterior EMG and measures of MAP which include; fascicle length (FL), pennation angle (PA) and muscle thickness (MT).

The results of an analysis of variance found a significant difference between joint angles for measures of FL and PA but not MT. A significant difference was found between probe rotations for the measures of FL and MT but not PA.

A reliability study was performed for measures of MAP and found the coefficient of variation for FL and PA to be less than 8% both with and without the use of an image filter. The coefficient of variation for MT was found to be less than 2% which shows this measure to be highly reliable.

Equations and Figures were developed, corresponding to the observations and assumptions made by MAP researchers using BMU, to predict the effect of probe orientation on the measures of MAP.

The results of this study indicate that ultrasound probe orientation affects measures of MAP but the effect either cannot be predicted from a simple geometric model or the error in the measurement technique does not allow this type of comparison.

Specific guidelines are outlined in this paper to determine the proper probe placement and orientation to measure MAP using BMU for the tibialis anterior muscle.

Table of Contents

List of Figures

List of Tables

Chapter 1. Introduction

Muscles are complex organs capable of producing force to stabilize and move body segments as well as absorb energy imparted to the body (Hawkins, 2000). It is widely accepted that the structure of muscle is associated with its mechanical action (Kawakami et al., 2000). The purpose of this section is to present work in the field of muscle mechanics that attempts to relate muscle structure to force transmission and production. The discussion will begin with a review of muscle anatomy. Next, a brief history of muscle mechanics research will be presented outlining major discoveries that relate muscle structure to function. Then, the use of Brightness-Mode ultrasonography (BMU) to measure Muscle Architecture Parameters (MAP) will be examined with specific focus on methodology. Finally, the rationale for an experiment to validate the use of BMU to measure MAP will be presented.

1.1. Muscle structure

Muscle structure can be defined by the arrangement of the functional contractile material relative to the supporting elastic structures (McComas, 1996). The sarcomere is considered to be the smallest functional unit of muscle (Lieber, 1999). Due to the peculiar structure and action of the sarcomere, the arrangement of sarcomeres in a muscle is considered to determine certain functional properties of that muscle (Wickiewicz et al., 1984; McComas, 1996; Fukunaga et al., 1997). Sarcomeres connected in series are believed to allow greater range of motion and shortening velocity, while sarcomeres

connected in parallel produce greater force (Lieber, 1999; Kawakami et al., 2000). A myofibril is a number of sarcomeres attached in series and a muscle fibre (muscle cell) is made of many myofibrils connected in parallel and covered in a collagen sheath.

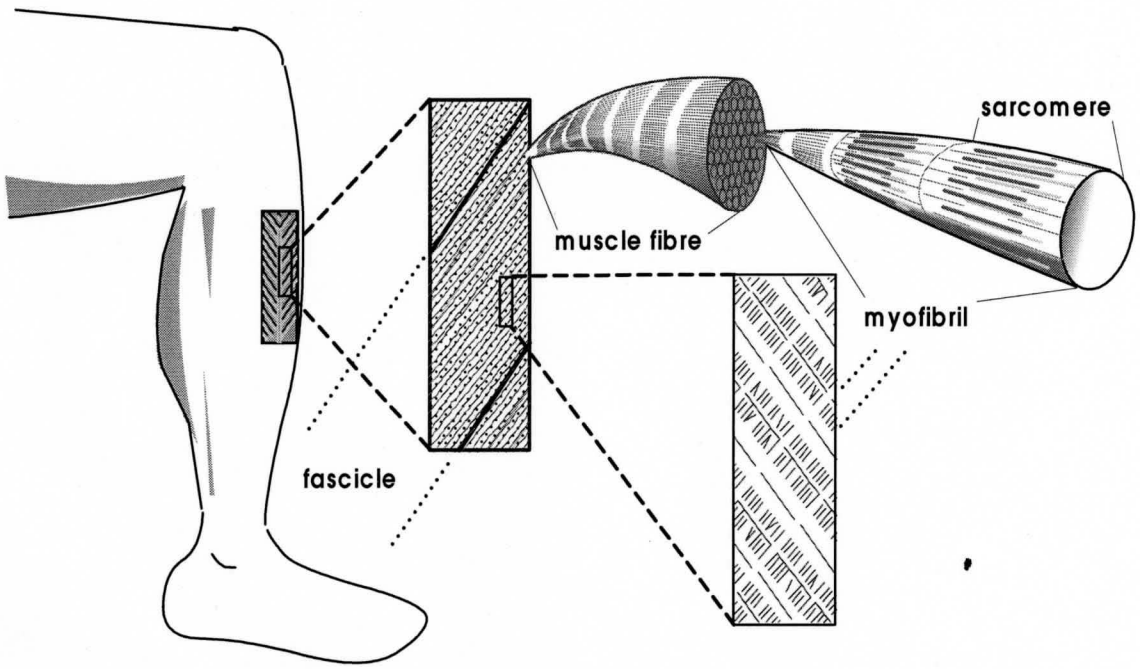

Figure 1-1 The levels of muscle organization.

Muscle architecture research is based on the theory that the length and arrangement of muscle fibres are important determinants of the whole muscle function (Delp et al., 2001). Muscle fibres packed in bundles and surrounded by a fascial sheath, (perimysium) make up a muscle fascicle (Lieber, 1999). A fusiform muscle is a muscle with fascicles that run parallel to the line of action of the muscle. The fascicles within a pennate muscle run at an angle to the line of action of the muscle attaching onto the supporting tendinous structures within and around a muscle. The angle at which the fascicles attach onto the tendinous structures is called the pennation angle (PA).

Aponeuroses are tendinous structures that run either internally or externally to a muscle and are normally continuations of the extra-muscular tendon (Nigg & Herzog, 1999). The structural arrangement of a pennate muscle is considered to be both advantageous and disadvantageous to force production (McComas, 1996; Fukunaga et al., 1997; Lieber, 1999; Kawakami et al., 2000). In pennate muscles there is an increase in the effective cross-sectional area due to the existence of more fibres in parallel (McComas, 1996; Fukunaga et al., 1997; Lieber, 1999; Kawakami et al., 2000). There is also an attenuation of the potential force of an individual fascicle due to the smaller component of force which is aligned with the line of action (McComas, 1996; Fukunaga et al., 1997; Lieber, 1999; Kawakami et al., 2000).

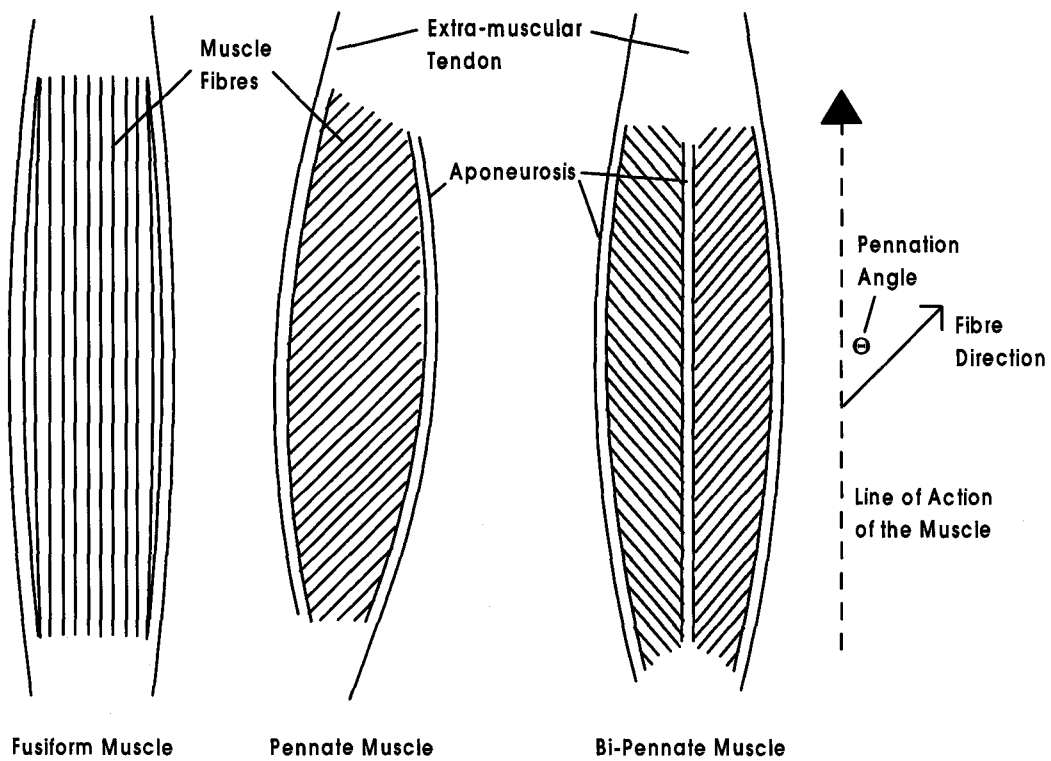

Figure 1-2 The arrangement of muscle fascicles.

Another important feature of pennate muscle is that the distance moved by the aponeurosis during contraction is greater than the amount of fibre shortening (McComas, 1996). This discrepancy between distances allows the fibres to function over the optimal part of their force-length curves (McComas, 1996).

The action of the fascicle is considered to be in direct relation to the action of the sarcomere. As the sarcomere contracts it creates tension which is transmitted to other sarcomeres or structures attached in series. The line of action of a fascicle is consistent with the line of action of the individual sarcomere. Therefore, the fascicle length (FL) and the angle with which the fascicles attach to the aponeurosis in a pennate muscle (pennation angle, PA) are determining factors of the force, length and velocity potential of the muscle (Wickiewicz et al., 1984; Maganaris et al., 1999). This is why the MAP of most interest to researchers are FL and PA. Muscle thickness (MT) is also an important architectural characteristic as it defines the distances between the aponeuroses.

1.2. Historical Observations

This section outlines some major discoveries that contribute to the present understanding of muscle mechanics and to the use of MAP to measure muscle function.

The force-velocity relation of muscle began with the work of Wallace Fenn (Hill, 1970). In 1924, Fenn found that the rates of the chemical reactions underlying contraction are controlled by the mechanical conditions (Fenn, 1924). In 1938, Fenn and Marsh produced a paper and an equation on the relation between the speed of muscle shortening and the force exerted (Fenn and Marsh, 1935). A.V. Hill, considered by many to be *the*

grand old man of muscle and nerve physiology (Huxley, 2000) attempted to continue Fenn's original line of research on the heat of shortening and the heat of activation of toad muscle (Hill, 1948). It was only when Hill began to develop an equation for his results that he found that the heat values he was using in his equation were proportional to the load (Hill, 1970). Hill's revised equation was much simpler than the equation that Fenn and Marsh had developed for the force-velocity relation but had the same results (Figure 1-3). Hill is therefore attributed with the discovery of a simple equation to determine the force-velocity relation of muscle from a few experimentally determined values (Huxley, 2000) (Figure 1-3). Other experiments using quick release to study the development of tension, the effect of shortening and lengthening muscles at various rates as well as his study of the visco-elastic response of a muscle to spring oscillations, would help Hill to develop a three component structural model of muscle (Hill, 1951; Huxley, 2000). Hill also aided in the development of a force-length relation and a force-history relation of muscle (Hill, 1970).

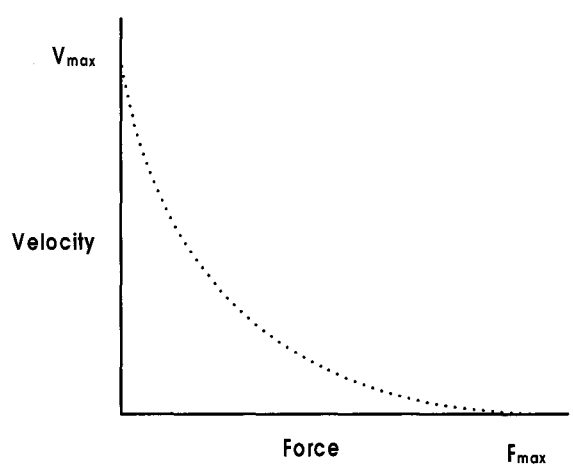

Equation for the Force-Velocity relation of muscle

$$v = b(F_{max}-F)/(F+a)$$

F = force
F_{max} = the maximum force at zero velocity
v = the shortening velocity
b = velocity constant
a = force constant

Figure 1-3 The force-velocity relation (adapted from Hill 1970)

The three component model of muscle states that a contractile unit lies in series with an elastic component and in parallel to another elastic component (Hill, 1950) (Figure 1-4). This model, along with the force-velocity relation, force-length relation and other muscle relationships, can be used to predict the action of muscle (Dowling, 1997). The contractile unit at the time was considered to be continuous protein chains that folded to produce tension (Huxley, 2000). The tendon was thought to be the series elastic component and the parallel elastic component was considered by Hill to be both within and around the contractile unit (Hill, 1950).

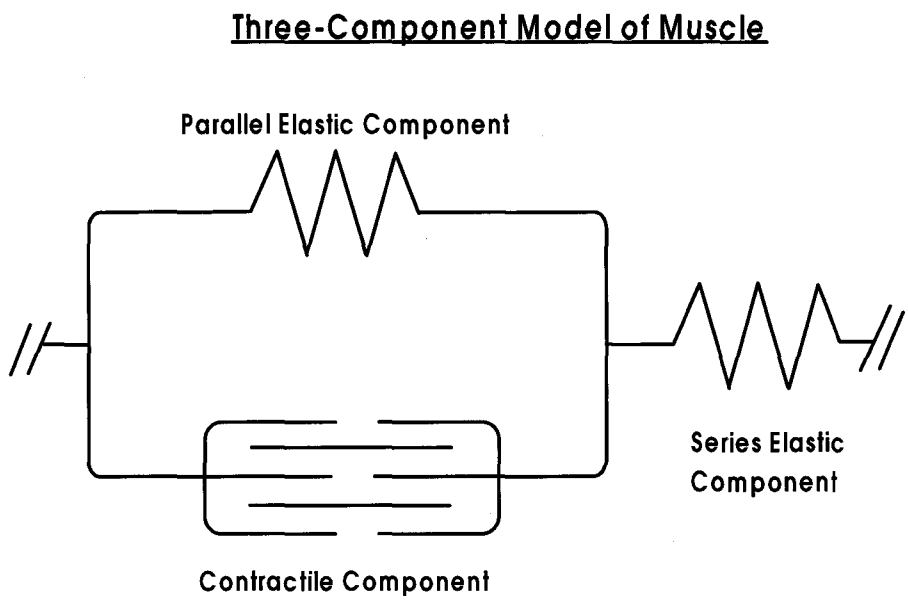

Figure 1-4 The Three component model of muscle.

The force-length relation of muscle was more extensively studied by Ramsey and Street (Ramsey and Street, 1940). In 1940, Ramsey and Street discovered that the tension developed by muscle depended on the muscle length. The relationship that they found

was only later explained by the structure of the sarcomere and the consideration of the three component model of muscle (Huxley, 2000).

The simultaneous discovery of the microscopic structure of the sarcomere by Hugh Huxley and Andrew Huxley and the resulting sliding filament theory have aided tremendously in the development of the field of muscle mechanics (Huxley & Hanson, 1954; Huxley & Niedergerke, 1954; Huxley, 2000). The sliding filament theory postulates that the force-length relation and force-velocity relation of muscle are due to the structure and action of the sarcomere (Huxley, 1957). Gordon, Huxley and Julian (1964) gave experimental evidence relating the force-length relation to the amount of actin and myosin overlap in the sarcomere (Figure 1-5). The force-velocity relation was considered to be caused by the rate of formation and breakdown of myosin cross-bridges (Huxley, 1957).

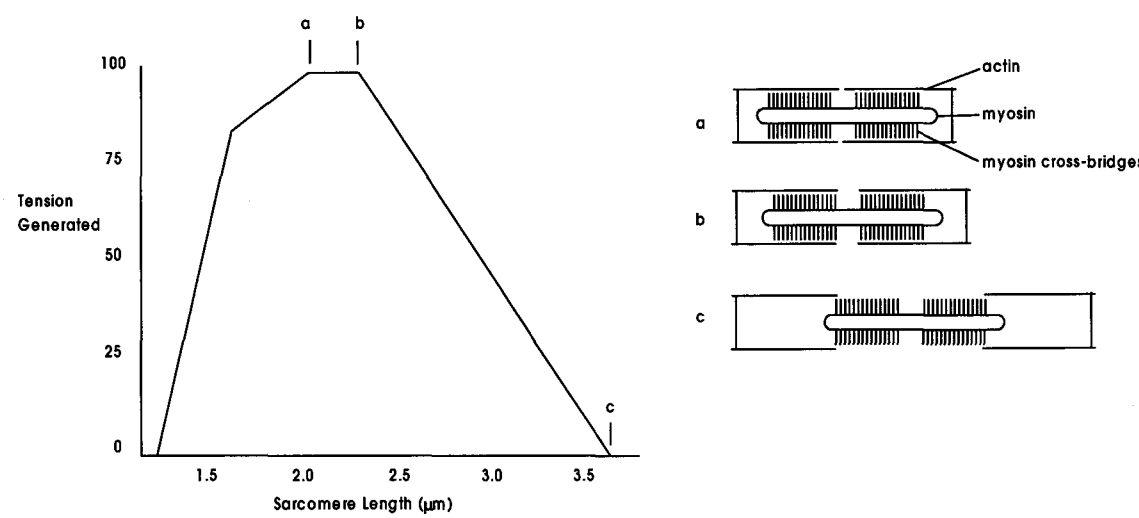

Figure 1-5 The force-length relation graph and representation of actin and myosin overlap that define the relationship. (adapted from Gordon 1966)

The passive material that constitutes the series and parallel elastic components of muscle may also play an important role in MAP research. In a review on the series and parallel elastic components of muscle from a material engineering perspective, Huijing (1999) challenges the pre-existing ideas about the use of muscle architecture to determine muscle function because of the potential for lateral force transmission through the muscles supporting structures. Huijing compares the microscopic structure of muscle to a composite which, in material engineering terms, is a material comprised of many different components (Huijing, 1999). Huijing considers muscle to be a composite consisting of an extracellular matrix with triple reinforcement by fibrous material. He contends that the reinforcement is obtained by (1) an active component (myofibers) (2) the basal lamina and (3) the passive fascial apparatus of the muscle (Huijing, 1999). Past experiments highlighted in this review include those by Street and Ramsey who show force transmission through damaged myofibrils. These studies show that force is not exclusively transmitted through sarcomeres in series (Street and Ramsey, 1965; Huijing, 1999). Recent experiments performed by Huijing show the effect of partial facsiatomies (surgically altering the supporting structure of the muscle) on force production in mammalian muscle (Huijing, 1999). These experiments show that when some myofibrils are no longer intact to the tendon or bone attachment the whole muscle is still able to produce a larger proportion of force than would be estimated without lateral force transmission (Huijing, 1999). Other important implications of these fasciatomy experiments show that the type of fasciatomy affects the level of force production through the whole muscle (Huijing, 1999). This helps to explain how the whole

architecture of the muscle is important in determining the force producing capability of the muscle (Huijing, 1999).

In summary, the experimentally developed relationship between muscle action and force has been linked to the structure and action of the smallest functional unit of contraction (the sarcomere). Since the fascicle structure is believed to be directly related to the structure of the sarcomere, it is theoretically feasible that force production in muscle can be determined by the architectural arrangement of fascicles within a muscle.

1.3. Methods of Determining Muscle Architecture Parameters

1.3.1. Cadaver studies

The first method used to determine MAP was through cadaver studies (Kawakami et al., 1993; Scott et al., 1993; Narici et al., 1996). This involved the manual measurement of FL and PA on dissected specimens. This is no longer an acceptable method of determining these parameters as MAP change throughout contraction in living tissue and the preparation of the cadavers shrinks the fibers, thereby changing the fibre orientation within the muscle (Kawakami et al., 1993; Narici et al., 1996).

1.3.2. Piezo-electric crystallography

Kaya et al. (2002) used piezo-electric crystals in an attempt to develop a model of the instantaneous contractile element length from force values. They found that the MAP to force relationship is a complex non-linear relationship. The technique of piezo-electric crystallography requires the placement and detection of tiny piezo-electric crystals on the

fascicle insertions within a living subject's muscle. This is an expensive technique which requires strict ethical supervision and has only been used on animals. Therefore this tool is not reasonable for large scale use.

1.3.3. Ultrasound to measure MAP

One of most prevalent techniques for imaging muscle architecture in-vivo has been through the use of Brightness-Mode ultrasonography (Kawakami et al., 2000; Maganaris et al., 2002). BMU uses the transmission and reflection of high frequency longitudinal, mechanical waves in tissue to develop a two-dimensional image on a computer display (Zagzebski, 1986). The ultrasound transducer is made of a material that can transform electrical impulses into mechanical waves (Fish, 1990). An ultrasound transducer is fitted with a transmitter and receiver so that it can both create and detect ultrasound waves (Fish, 1990). Most transducers have a piezo-electric element that produces the ultrasound wave (Fish, 1990). The transmitter controls the duration and frequency of the wave through the use of a timer (Fish, 1990) causing short bursts of ultrasound waves which determines the pulse repetition rate of the wave (Fish, 1990). This rate allows the eventual image to be constantly refreshed so as to detect movement (Fish, 1990).

The ultrasound wave originates from the ultrasound transducer and travels through a medium at a speed which depends on the complexity and density of the medium (Fish, 1990). The speeds in different soft tissues vary but are approximately 1540 m/s. (Fish, 1990). At a boundary between two tissues some ultrasound passes

through the boundary and some is reflected. The magnitude of this reflection depends on the acoustic impedance of the two tissues (Fish, 1990). A large difference in acoustic impedance leads to a large magnitude of reflection (Fish, 1990). A reflected wave that returns to the transducer is called an echo (Zagzebski, 1986). The time of transmission and arrival of a reflected echo can be converted to the distance from the interface to the transducer. This is achieved by calibrating the transducer for the velocity of sound of the medium being examined. Only echoes returning to the probe within the ultrasound beam will be detected by the transducer/reciever (Zagsebski, 1986). The ultrasound beam is the region where the longitudinal waves produced by the ultrasound transducer exist as they travel out from the transducer. The geometry of the ultrasound beam is determined by the size and shape of the ultrasound probe as well as its frequency of operation (Zagsebski, 1986). A single piezo-electric disc element creates an ultrasound beam with a near field, a focal field and a far field whose size and dimensions depend on the size and curvature of the disc. The ultrasound wave is strongest in the centre of the beam and diminishes towards the edges (Fish, 1990). A linear array probe is created by stacking many piezo-electric elements to create an ultrasound beam that can reliably determine real life dimensions (Fish, 1990). Muscle imaging experiments require linear array transducers (Kawakami et al., 2000)(Figure 1-6).

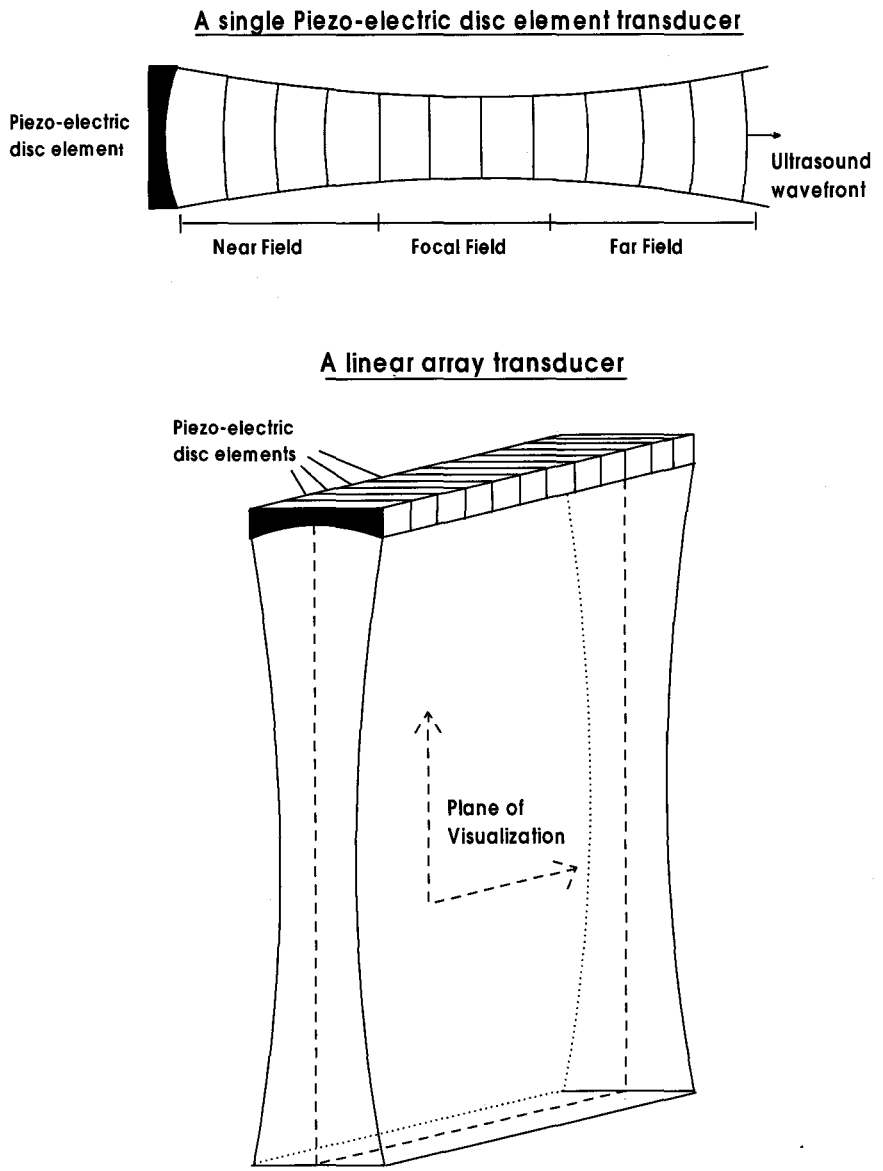

Figure 1-6 The diagrammatic representation of an ultrasound beam from a single piezo-electic disc and the linear array transducer.

The ultrasound beam produced by a linear array probe can also be referred to as a plane of visualization. The plane of visualization obtained through the use of a linear array ultrasound transducer allows the researcher to assume that the image displayed has dimensions relative to the plane of contraction of the muscle and therefore allows the

researcher to conduct a two-dimensional kinematic analysis of the MAP (Kawakami et al., 2000). Calibration of the ultrasound probe can be achieved by imaging wire frames of known dimensions in a liquid bath (Fish, 1990).

A two-dimensional ultrasound image is built by displaying each reflected echo from tissue as a dot on a computer screen. The intensity (grayscale) of the dot is determined by the strength of the echo and the location of the echo is dictated by the position of the ultrasound beam and the time of arrival of the echo (Zagzebski, 1986).

The spatial resolution of the ultrasound image depends on the frequency of operation of the ultrasound transducer. Ultrasound is attenuated as it passes through tissue (Fish, 1990). Different tissues attenuate ultrasound to a different degree (Fish, 1990). The attenuation of ultrasound increases with the frequency of the wave and the choice of wave frequency depends on the requirement of resolution and depth of the image (Fish, 1990).The ability to resolve close images requires a high frequency while high penetration requires a low frequency (Fish, 1990). Probes used for muscle imaging have frequencies of operation between 5-10 MHz, these are considered to be high frequencies chosen for their spatial resolution (Herbert et al., 1995; Narici et al., 1996; Kawakami et al., 2000; Maganaris et al., 2002).

B-mode ultrasonography also allows the researchers to obtain real-time images up to 65 Hz frame rate (Kawakami et al., 2002). Real time scanners sweep the ultrasound beam periodically through the region of interest at a sufficiently high rate to visualize tissue movement as it occurs (Fish, 1990).

1.3.3.1.Images

The images developed from BMU only show specific structures with high reflective qualities. The structures within the muscle that reflect the ultrasound waves and are therefore visualized are, the epimysium, which is the collagen connective tissue that covers the surface of the muscle. The perimysium, also made of collagen, is the sheath-like structure that wraps muscle fibres in bundles to form fascicles and has also been called fascia. Other structures observed using BMU are any tendon-like structures, such as deep and superficial aponeuroses. It is important to note the muscle fibres themselves are not clearly visualized due to small differences in acoustic impedance and it is assumed that the movement of the visualized fascia can be considered a direct representation of the muscle it surrounds (Herbert et al., 1995; Narici et al., 1996; Kawakami et al., 2000; Maganaris et al., 2002).

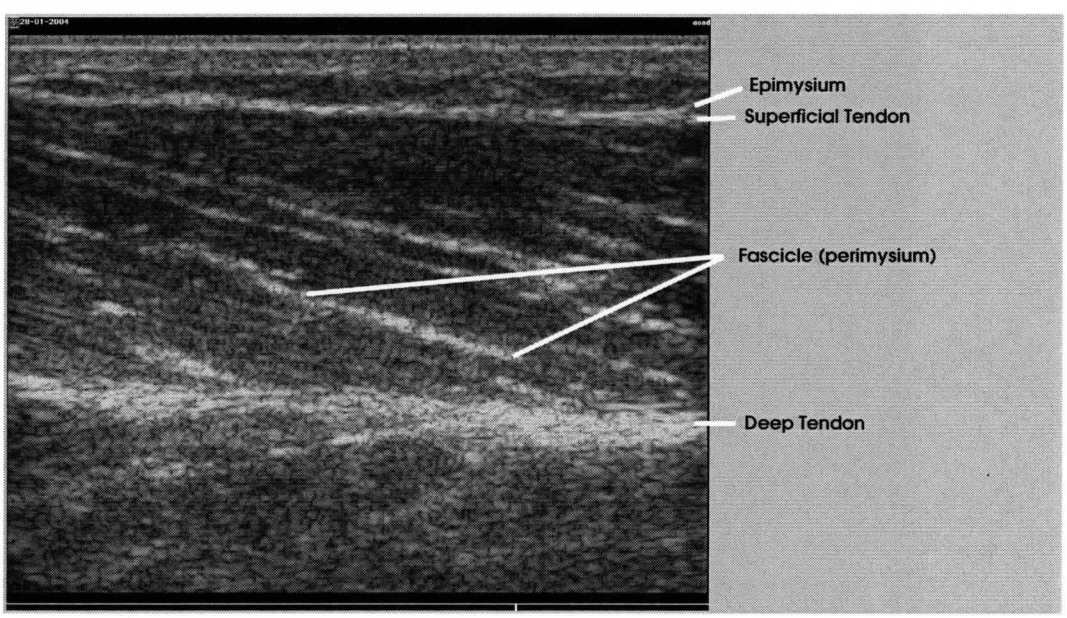

Figure 1-7 An ultrasound image showing specific visualized structures

1.4. Current MAP research using Ultrasound

Ultrasound is currently used to study MAP's in an attempt to relate and determine the functional characteristics of muscle that are still relatively unknown. For example, Hodges et al. (2003) observed that ultrasound imaging can be used to detect low levels of muscle activity, as measured by EMG, but cannot discriminate between moderate and strong contractions. For the tibialis anterior, Hodges et al. (2003) found that PA could reliably detect a change in EMG of 9% while FL and MT could predict a change in EMG of 16%.

Reeves et al. (2003) studied the effect of different angular velocities on measures of MAP for both concentric and eccentric contractions and concluded that a constant fibre length cannot be assumed from the same joint angle during concentric contractions of different angular velocities.

Maganaris et al. (2002) used ultrasonography to assess the effects of repeated maximum isometric contractions on the geometry of gastrocnemius muscle. Maganaris et al. (2002) found that the greatest change in muscle architecture occurred after the first contraction. They associated the change in MAP to tendon creep (Maganaris et al., 2002). Maganaris et al. (1999) has also attempted to develop a predicted planimetric model of PA change to determine ankle joint angle change in the tibialis anterior muscle.

Kawakami et al. (2002) used the change in MAP during a countermovement action to validate a theory of muscle-tendon interaction that describes a mechanism for the increased force experienced in a countermovement action. Kawakami et al. (2002) measured fascicle lengths from ultrasound images obtained during a countermovement

and a non countermovement action and discussed the changes in the whole muscle tendon unit relative to the length change of the fascicle.

Studies by Kawakami et al. (1993) and Aargaard et al. (2001) observed an increase in PA following training. This increase in pennation is considered a potential mechanism for the increase in strength of the participants (Kawakami et al., 1993; Aargaard et al., 2001)

All of these studies rely upon the current understanding of the measurement technique. Therefore, the technique must be thoroughly investigated to determine any issues that could result in measurement errors.

1.5. Ultrasound research

The purpose of the current section is to present specific methods and assumptions made by researchers using the tool of the BMU in the measurement of MAP. The discussion of the BMU research will focus on;

1. How MAP are measured in different experiments
2. Ultrasound probe placement
3. Reliability of the measurement technique
4. How the experimenters considered potential muscle or probe rotation

The three most common MAP measured are fascicle length (FL), pennation angle (PA) and muscle thickness (MT). Each of these MAP will be discussed as to how they are currently measured.

The measurement of FL has been conducted three different ways. The first method of measuring FL is based on the assumption that a fascicle is straight and the distance from the insertion of that fascicle from the deep to the superficial aponeurosis is determined (Narici et al., 1996). A second method is based on the assumption that the fascicle is curved and therefore the length of the fascicle is measured along its path (Kawakami et al., 2000). The last way of measuring FL is by using the measured PA, assuming a straight fascicle, and applying trigonometry to solve for the FL (Maganaris et al., 1999; Reeves et al., 2003). The trigonometric method is used when the insertion of the fascicle into the deep or superficial aponeurosis can not be visualized on the image. Occasionally all three of these methods are used in the same study when either there is a clear curvature to the fascicle or the insertion into the deep or superficial aponeurosis is not clearly seen on the image (Reeves et al., 2003). The predicted FL from trigonometry has also been tested against actual measurements and found to be within 2.4% of the actual value for the tibialis anterior muscle (Reeves et al., 2003).

The measure of PA in a bi-pennate muscle is consistently determined as the average of the angles between the measured fascicle and the deep and superficial aponeurosis assuming a straight fascicle. When the fascicle is curved, the PA is taken from a straight line drawn from the insertion point of a fascicle along the curve of the part of the fascicle closest to the aponeurosis of interest (Maganaris et al., 1999; Kawakami et al., 2000; Reeves et al., 2003).

MT is defined as the average perpendicular distance between the aponeurosis as measured on either end of the image (Maganaris et al., 1999; Kawakami et al., 2000; Reeves et al., 2003).

The methods currently used required the experimenter to manually measure PA, FL , and MT, using an image analysis program. The major error associated with this type of measurement is due to human error. The ultrasound images lack the clarity necessary to distinguish definitive areas of transition from one structure to the next and these areas of transition make it difficult to determine reliable start and end points for measurement. Most studies to date have included an analysis of the reliability of their measurement technique (Maganaris et al., 1998; Reeves et al., 2003; Fukunaga et al., 1997). The coefficient of variation from the studies ranges from 0.5 to 9.8 % (Fukunaga et al., 1997; Maganaris et al., 1998; Reeves et al., 2003).

Because the ultrasound technique of muscle imaging restricts the analysis of muscle FL and PA to a 2D kinematic analysis, great detail has been taken in the preparation and imaging of specific muscles to validate that the plane of visualization is consistent with the plane of contraction. This issue should be considered with respect to probe placement, which is the probe/skin interface on the surface of the skin over a muscle, and probe orientation, which is the rotation of the ultrasound probe in the transverse and frontal plane once a probe placement has been chosen.

Narici et al. (1996) used a cadaver specimen to verify the correct orientation of an ultrasound transducer necessary to visualize the muscle architecture of the human gastrocnemius muscle. They found that the gastrocnemius muscle architecture could be

viewed properly by orienting the transducer along the median longitudinal axis of the muscle (Narici et al., 1996). This axis is determined by marking the distal end of the muscle belly and the proximal tendon and by drawing a straight line connecting these sites. Also by imaging many sites along and parallel to this line, Narici et al. (1996) found that measurements performed along the mid-sagittal axis were representative of the medial gastrocnemius architecture at rest and in the contracted state.

Herbert and Gandevia (1995) used ultrasonography to visualize the brachialis muscle architecture in an elbow flexion and extension task. By visualising different sites along the brachialis muscle Herbert and Gandevia (1995) concluded that the fascicle behaviour remained consistent between imaging sites. Herbert and Gandevia (1995) used three transducer locations in their study of the brachialis muscle and found consistent results between locations. They concluded that the placement of the transducer does not alter the potential results and that the observed changes in PA with elbow torque and elbow angle are not an artifact produced by rotation of the muscle relative to the transducer. In their study, Herbert and Gandevia (1995) also noticed that a rotation of the ultrasound probe by greater than 5 degrees markedly distorted the image produced by the ultrasound computer. This suggests that a 10 degree window exists where measures of MAP can be performed at a given probe placement and introduces the potential importance in considering probe orientation as a factor in MAP measurement using BMU.

When attempting to image the architecture of the triceps surae muscles during contraction, Kawakami et al. (2000) noticed that in order to correctly measure the lengths

of the fascicles, it was important to line up the plane of the ultrasonogram with the plane of the fascicles which was achieved by changing the plane of the ultrasonogram slightly diagonally to the longitudinal line of the muscle so that the FL was not overestimated and the fascicle angle was not underestimated. This assumes that the correct plane of visualization can be determined by finding the smallest measure of FL with the greatest measure of PA. Reeves et al. (2003) noticed that the tibialis anterior (TA) muscle does not act solely in a sagittal plane and this may result in scanning the muscle from a slightly different orientation, resulting in the appearance of an increased distance between aponeuroses. The issue of probe orientation has only been mentioned in these articles and no studies have been conducted analyzing the potential error that could result from probe orientation.

Kawakami et al. (2000) used a magnetic tracking device to develop a three dimensional reconstruction of fascicles from ultrasound images. From this study they concluded that FL remained uniform in the medial gastrocnemius in both a contracted and relaxed state. Ultrasonic images were obtained from eight positions on the medial gastrocnemius parallel to the longitudinal axis of the muscle. The imaged sites were separated by one fourth of the width (mediolaterally) and by one third of the longitudinal length (from midbelly to the distal end) (Kawakami et al., 2000). One of the possible limitations of the study is that the fascicle is always assumed to lie perpendicular to the ultrasound beam and to be the shortest distance between muscle boundaries. Furthermore, this reconstruction was taken during an isometric contraction and the original position of

the fascicles is not known. Therefore, potential rotation of the muscle or the transducer during contraction can not be assessed.

The use of ultrasound to measure MAP is relatively new and the techniques of measurement now rely heavily upon these papers to validate the measure of MAP with two-dimensional ultrasound. The results from these studies indicate that probe placement on the muscle does not affect the measurement of MAP. However, as Kawakami et al. (2000) have noticed, there can be distortion of the image of the muscle due to the orientation of the probe regardless of the probe placement. This orientation issue is important for researchers to consider in determining the correct guidelines for muscle architecture research using B-Mode ultrasonography.

1.6. Development of Equations

In order to determine the error that could result from probe orientation, on the measures of MAP from ultrasound images, a series of figures and theoretical equations was developed. The following figures show the effect of transverse and frontal rotation of the ultrasound transducer on the resulting measurement of MAP. These rotations are assumed to mimic the potential rotation an investigator would perform while attempting to properly visualize MAP. The axes of rotation are located at the skin/probe interface and the muscle is assumed to be a rectangular prism with fascicles running the shortest distance between muscle boundaries (Narici et al., 1996; Kawakami et al., 2000). Narici et al. (1996) found that, in the medial gastrocnemius, the fascicles take essentially a parallel course with respect to the longitudinal axis of the muscle. A longitudinal slice of

a cadaver specimen was made to compare the BMU measurements to actual measurements of MAP (Narici et al., 1996).

The 3 dimensional orientation of a fascicle within muscle has been studied in the past with the use of MRI (Scott et al., 1993). Scott et al. (1993) used frontal and sagittal plane projections of FL from MRI images to predict the 3 dimensional orientation of the fascicle in the muscle. The vastus lateralis was studied and it was found that the orientation of the fascicles remained consistent throughout the muscle. They found that the true length of the fascicle could be assumed from a two-dimensional cross section of the muscle visualized from an oblique plane. The present study is based on the assumption that there is a correct plane of contraction which can properly estimate the actual FL. The plane of contraction is the two dimensional cross section which accurately represents the length of the fascicle (Figure 1-8). This is considered to be consistent to observations made by Kawakami et al. (1993) and Reeves et al. (2003).

The orientation of the ultrasound probe and the resulting image is portrayed in Figure 1-8 (left). A single fascicle is shown in Figure 1-8(right) as a three-dimensional line segment. With the fascicle represented as a three dimensional line segment equations can be developed to determine the fascicles length and angle of pennation (Equation 1-1, Equation 1-3). The end points of the fascicle line segment are three dimensional coordinates such as (x_1,y_1,z_1) corresponding to a point position. The effect of transverse and frontal rotation of the probe and the resulting fascicle end points are illustrated in Figures; 1-9, 1-10, and 1-11. The transverse and frontal rotation of the probe and the new fascicle lengths require new equations to be developed to represent the new fascicle

length, pennation angle and muscle thickness (Equation 1-4,1-5,1-6,1-7,1-8,1-9,1-10,1-11,1-12).

The predicted equations are based on the assumption that the muscle structure can be treated like a rectangular prism for the small rotations achieved in this study. If the plane of contraction provides the proper dimensions to measure FL, then rotation of the plane of visualization, developed by the ultrasound beam, in the transverse and frontal planes would result in an inaccurate representation of MAP values. Therefore the proper plane of contraction could be determined as the plane that visualizes the smallest measure of FL. These equations and figures will be compared to actual values to determine if a proper plane of contraction can be determined. The equation developed to allow for both y (transverse) and z (frontal) axis rotation will be used to determine how the actual measurement of MAP compare to predicted values.

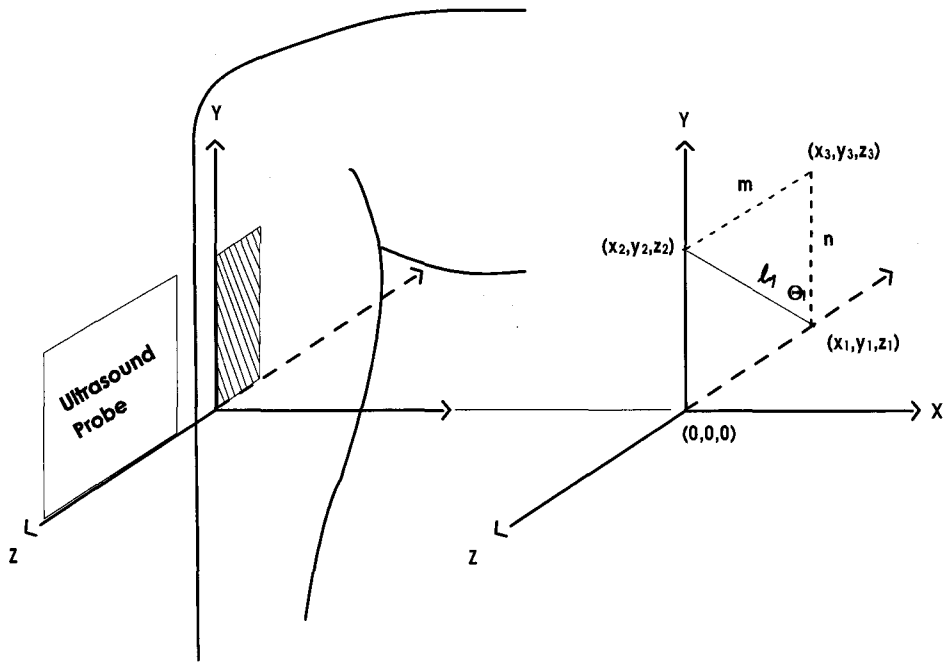

Equation 1-1

$$\text{Fascicle Length} = l_1$$
$$= |(x_1,y_1,z_1) - (x_2,y_2,z_2)|$$
$$= |(0,0,-m) - (0,n,0)|$$
$$= |(0,-n,-m)|$$
$$= \sqrt{(0)^2 + (-n)^2 + (-m)^2}$$

Equation 1-2

$$\text{Muscle Thickness} = (|(x_3,y_3,z_3) - (x_2,y_2,z_2)| + |(x_1,y_1,z_1) - (0,0,0)|)/2$$
$$= (|(0,n,-m)-(0,n,0)| + |(0,0,-m)-(0,0,0)|)/2$$
$$= (|(0,0,-m)| + |(0,0,-m)|)/2$$
$$= (\sqrt{(m)^2} + \sqrt{(m)^2})/2$$
$$= m$$

Equation 1-3

$$\text{Pennation Angle} = \Theta_1$$

$$|(x_3,y_3,z_3) - (x_2,y_2,z_2)|^2 = |(x_1,y_1,z_1) - (x_3,y_3,z_3)|^2 + |(x_1,y_1,z_1) - (x_2,y_2,z_2)|^2$$
$$-2|(x_1,y_1,z_1) - (x_3,y_3,z_3)||(x_1,y_1,z_1) - (x_2,y_2,z_2)|\cos\Theta_1$$
$$|0,0,-m|^2 = |0,-n,0|^2 + |0,-n,-m|^2 - 2|0,-n,0||0,-n,-m|\cos\Theta_1$$

Figure 1-8 Dimensions and equations to determine Muscle Architecture Parameters.

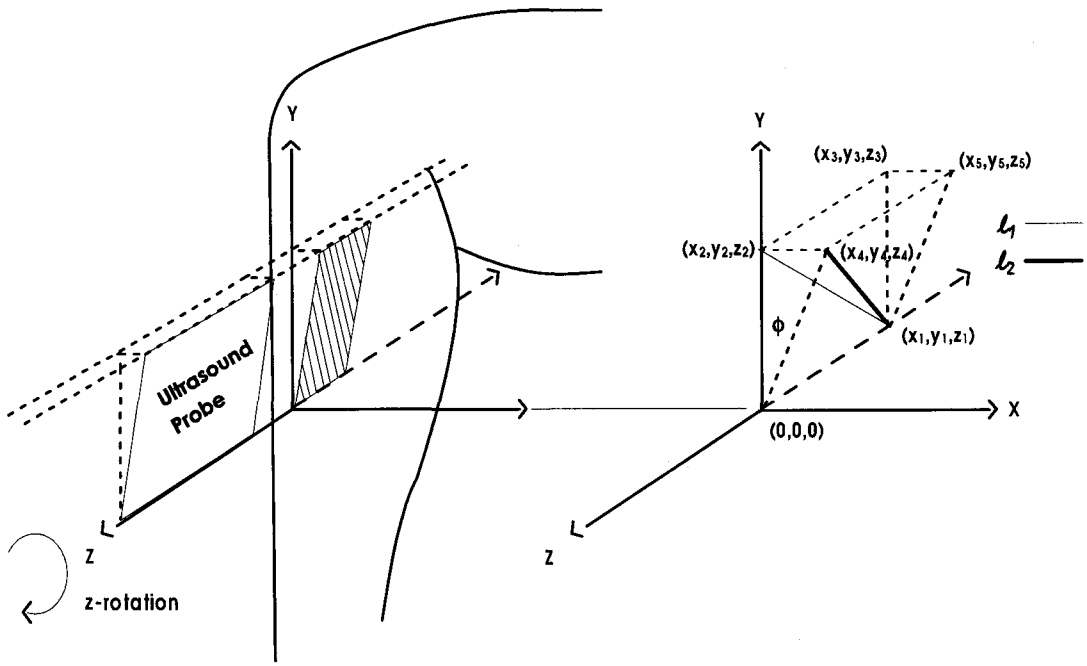

Equation 1-4

$$\text{Fascicle Length} = \ell_2$$
$$= |(x_1,y_1,z_1) - (x_4,y_4,z_4)|$$
$$= |(0,0,-m) - (n\tan\phi,n,0)|$$
$$= |(-n\tan\phi,-n,-m)|$$
$$= \sqrt{(-n\tan\phi)^2 + (-n)^2 + (-m)^2}$$

Equation 1-5

$$\text{Muscle Thickness} = (|(x_5,y_5,z_5) - (x_4,y_4,z_4)| + |(x_1,y_1,z_1) - (0,0,0)|)/2$$
$$= (|(n\tan\phi,n,-m) - (n\tan\phi,n,0)| + |(0,0,-m) - (0,0,0)|)/2$$
$$= (|(0,0,-m)| + |(0,0,-m)|)/2$$
$$= (\sqrt{(m)^2} + \sqrt{(m)^2})/2$$
$$= m$$

Equation 1-6

$$\text{Pennation Angle} = \Theta_2$$

$$|(x_5,y_5,z_5) - (x_4,y_4,z_4)|^2 = |(x_1,y_1,z_1) - (x_5,y_5,z_5)|^2 + |(x_1,y_1,z_1) - (x_4,y_4,z_4)|^2 - 2|(x_1,y_1,z_1) - (x_5,y_5,z_5)||(x_1,y_1,z_1) - (x_4,y_4,z_4)|\cos\Theta_2$$

$$|0,0,-m|^2 = |n\tan\phi,0,0|^2 + |n\tan\phi,-n,-m|^2 - 2|n\tan\phi,0,0||n\tan\phi,-n,-m|\cos\Theta_2$$

Figure 1-9 The predicted effect of z-rotation on the dimensions and equations to determine Muscle Architecture Parameters.

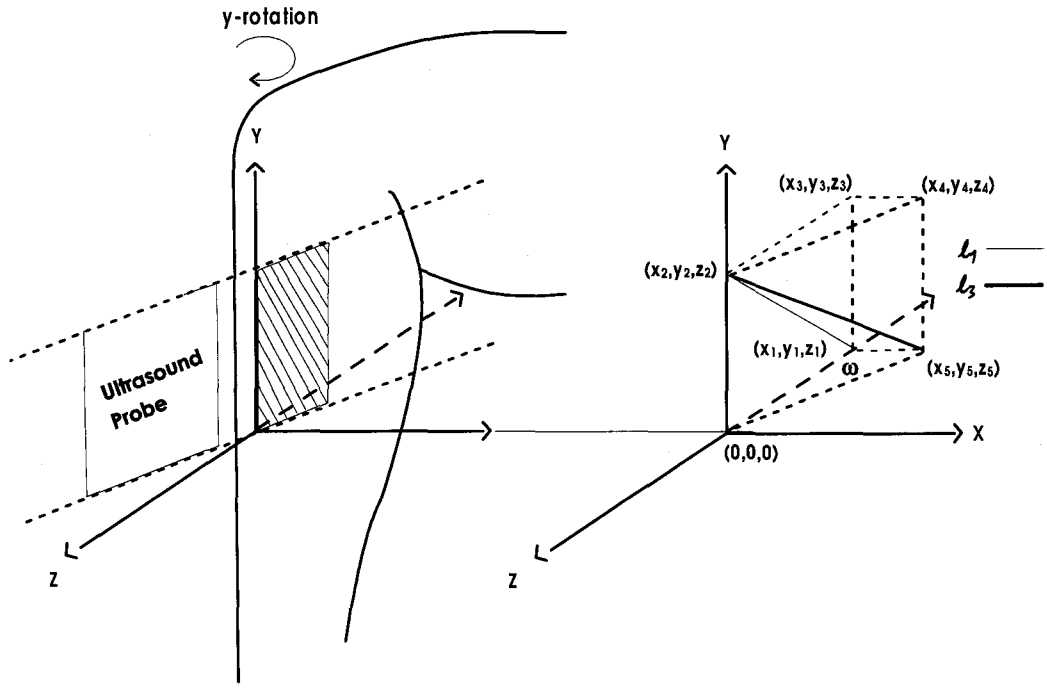

Equation 1-7

$$\text{Fascicle Length} = \ell_3$$
$$= |(x_5,y_5,z_5) - (x_2,y_2,z_2)|$$
$$= |(m\tan\omega 0,-m) - (0,n,0)|$$
$$= |(m\tan\omega - n,-m)|$$
$$= \sqrt{(m\tan\omega)^2 + (-n)^2 + (-m)^2}$$

Equation 1-8

$$\text{Muscle Thickness} = (|(x_5,y_5,z_5) - (0,0,0)| + |(x_4,y_4,z_4) - (x_2,y_2,z_2)|)/2$$
$$= (|(m\tan\omega 0,-m) - (0,0,0)| + |(m\tan\omega n,-m) - (0,n,0)|)/2$$
$$= (|(m\tan\omega 0,-m)| + |(m\tan\omega 0,-m)|)/2$$
$$= (\sqrt{(m\tan\omega)^2+(0)^2+(-m)^2} + \sqrt{(m\tan\omega)^2+(0)^2+(-m)^2})/2$$
$$= \sqrt{(m\tan\omega)^2+(0)^2+(-m)^2}$$

Equation 1-9

$$\text{Pennation Angle} = \Theta_3$$

$$|(x_4,y_4,z_4) - (x_2,y_2,z_2)|^2 = |(x_5,y_5,z_5) - (x_4,y_4,z_4)|^2 + |(x_5,y_5,z_5) - (x_2,y_2,z_2)|^2$$
$$-2|(x_5,y_5,z_5) - (x_4,y_4,z_4)||(x_5,y_5,z_5) - (x_2,y_2,z_2)|\cos\Theta_3$$
$$|m\tan\omega 0,m|^2 = |0,-n,0|^2 + |m\tan\omega,-n,-m|^2$$
$$-2|0,-n,0||m\tan\omega,-n,-m|\cos\Theta_3$$

Figure 1-10 The predicted effect of y rotation on the dimensions and equations to determine Muscle Architecture Parameters.

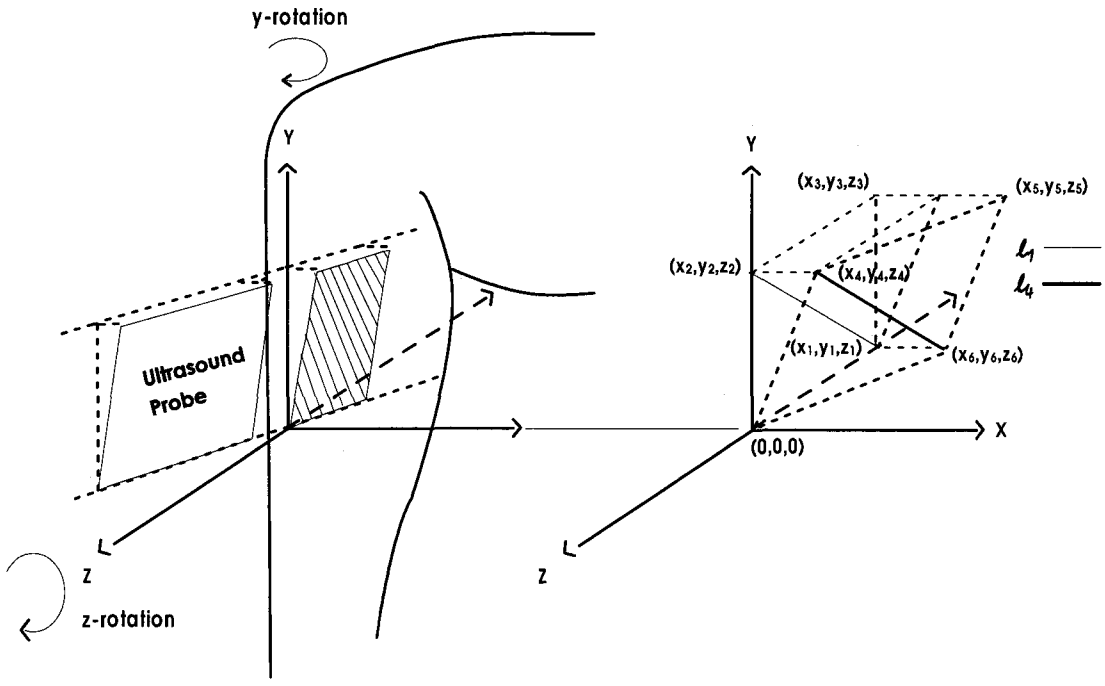

Equation 1-10

$$\text{Fascicle Length} = l_4$$
$$= |(x_6,y_6,z_6) - (x_4,y_4,z_4)|$$
$$= |(m\tan\omega 0,-m) - (n\tan\phi n,0)|$$
$$= |(m\tan\omega - n\tan\phi,-n,-m)|$$
$$= \sqrt{(m\tan\omega - n\tan\phi)^2 + (-n)^2 + (-m)^2}$$

Equation 1-11

$$\text{Muscle Thickness} = (|(x_5,y_5,z_5) - (x_4,y_4,z_4)| + |(x_6,y_6,z_6) - (0,0,0)|)/2$$
$$= (|(n\tan\phi + m\tan\omega n,-m) - (n\tan\phi n,0)| + |(m\tan\omega 0,-m) - (0,0,0)|)/2$$
$$= (|(m\tan\omega 0,-m)| + |(m\tan\omega 0,-m)|)/2$$
$$= (\sqrt{(m\tan\omega)^2+(0)^2+(-m)^2} + \sqrt{(m\tan\omega)^2+(0)^2+(-m)^2})/2$$
$$= \sqrt{(m\tan\omega)^2+(0)^2+(-m)^2}$$

Equation 1-12

$$\text{Pennation Angle} = \Theta_4$$

$$|(x_5,y_5,z_5) - (x_4,y_4,z_4)|^2 = |(x_6,y_6,z_6) - (x_5,y_5,z_5)|^2 + |(x_6,y_6,z_6) - (x_4,y_4,z_4)|^2 - 2|(x_6,y_6,z_6) - (x_5,y_5,z_5)||(x_6,y_6,z_6) - (x_4,y_4,z_4)|\cos\Theta_4$$

$$|m\tan\omega 0,-m|^2 = |n\tan\phi n,0|^2 + |m\tan\omega - n\tan\phi n,-m|^2 - 2|n\tan\phi n,0||m\tan\omega - n\tan\phi n,-m|\cos\Theta_4$$

Figure 1-11 The predicted effect of z-rotation and y rotation on the dimensions and equations to determine Muscle Architecture Parameters.

1.8. Purpose and Rationale for the study

The purpose of the present study is to determine the actual effects of transverse and frontal probe rotation on the measurement of MAP. This is believed to be important to (1) validate the two-dimensional method of measurement (2) present a potential basis with which to study the three-dimensional behaviour of muscle and (3) determine the errors that may be present in the current use of this tool. It is now quite difficult to establish a model of muscle force based on muscle architecture parameter measurements (Kaya et al., 2002; Hodges et al., 2003). Validating this tool or determining errors in the measurement may present an important observation that could help to improve the development of models or allow researchers to attempt new methods.

Because the experiment is restricted to using one probe it was necessary to be able to reproduce as many identical contractions of a muscle while maintaining a constant probe/skin interface and altering the probe orientation for each identical contraction. The end result of this design was the eventual comparison of the images produced from each contraction as if it were a different view of the same contraction, similar to a situation where one contraction was viewed with many probes. The experimental set-up required a constrained movement of a segment with a probe holding apparatus that maintained a constant probe/skin interface while allowing both transverse and frontal probe rotation. The muscular contraction was considered identical through the measurement of torque and the electromyographic signal of the muscle throughout the movement. The tibialis anterior muscle was chosen as it is 1) a clearly visualized muscle 2) the movement of the

muscle could be easily constrained and 3) the probe/skin interface would not be affected by contraction.

1.9. Limitations of the Study

Due to the relative infancy of MAP measurement using BMU, there is very little published research. For this reason it will be difficult to generalize the results from and to different muscles. Therefore it is most likely necessary to reproduce this experiment for many different muscles especially those used for muscle architecture parameter research.

Chapter 2. Methods

2.1. Subjects

This study involved nine subjects ranging in age from 22-45 yrs. One female and eight males participated in this study. Participants were recruited verbally. Verbal and written instructions about the protocol of the experiment were given to all participants. Each subject gave signed consent before participating in the study. This investigation was approved by the President's Committee on Ethics of Research on Human Subjects at McMaster University on Dec 15, 2003.

2.2. Experimental Setup

A plantar/dorsi-flexion boot was fitted with a single turn potentiometer to measure angular displacement. A weight stack was attached via a steel cable to provide a variable load as shown in Figure 2-1. The lower leg was stabilized to only allow for free ankle dorsi-flexion and plantar-flexion.

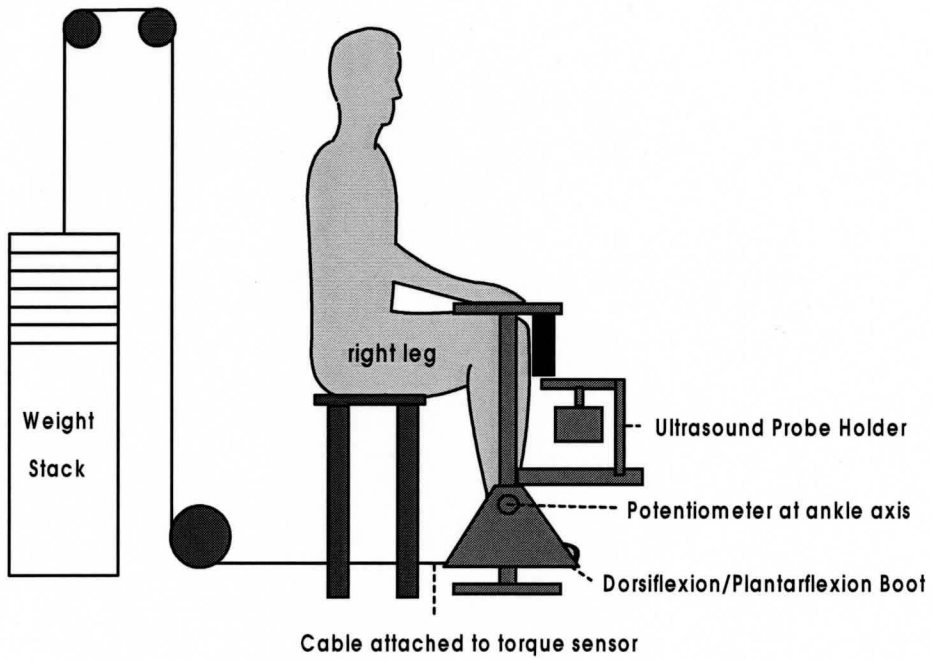

Figure 2-1 The experimental apparatus.

The cable was attached to a torque transducer connected to the bottom of the foot plate. This allowed the investigator to determine the load during the investigation. Electrical activity of the tibialis anterior muscle was recorded using Delsys dry-surface electromyography (EMG) electrodes. Ultrasound images were obtained using a 10MHz linear array probe attached to a General Electric^{TM} VingMed System-Five ultrasound device. The probe was placed in an apparatus designed to allow rotation about the transverse and frontal planes. This apparatus was attached to the front of the boot to allow the probe to visualize the tibialis anterior muscle.

2.2.1. Potentiometer

A single turn precision potentiometer was attached to one of the supporting beams of the boot and a two gear system connected the potentiometer to one of the bearings on the boot corresponding to the ankle joint of the subject. This two gear system was developed to allow for free movement of the bearing and potentiometer as well as to increase the range of the potentiometer.

2.2.2. Torque Transducer

The Torque transducer was mounted on a connecting beam on the bottom of the boot. The distance of the applied force to the boot ankle axis was 22.5 cm. The transducer was calibrated by hanging masses onto the attachment point of the cable on the boot. The boot was reoriented so that the force could be applied with the moment arm parallel to the floor. Actual torque was plotted against the computer values and a scaling factor of 0.1799 was calculated as the slope of the line of best fit. This value was multiplied by the measured torque in the experiment to place each value in units of Newton metres.

A scaling factor was also determined for volts so that a voltage signal from an oscilloscope could be used to calculate the 50% load used for each subject for the 9 slow-dorsi-flexion trials. The scaling factor was calculated to be 37.517 and was multiplied by the change in voltage from the maximum isometric dorsi-flexion trial to obtain the maximum load for each subject. This maximum load was multiplied by 0.5 to obtain a 50% load which would be used for the 9 slow concentric contractions. Because of the

restrictions of the weight stack, the loads used for each subject was closer to 45% of their maximum. The average % load was determined to be 43.5 ± 0.9 %

2.2.3. Probe Holder

An apparatus was designed to securely hold the ultrasound probe at various rotations about the transverse and frontal plane. (Figure 2-2)

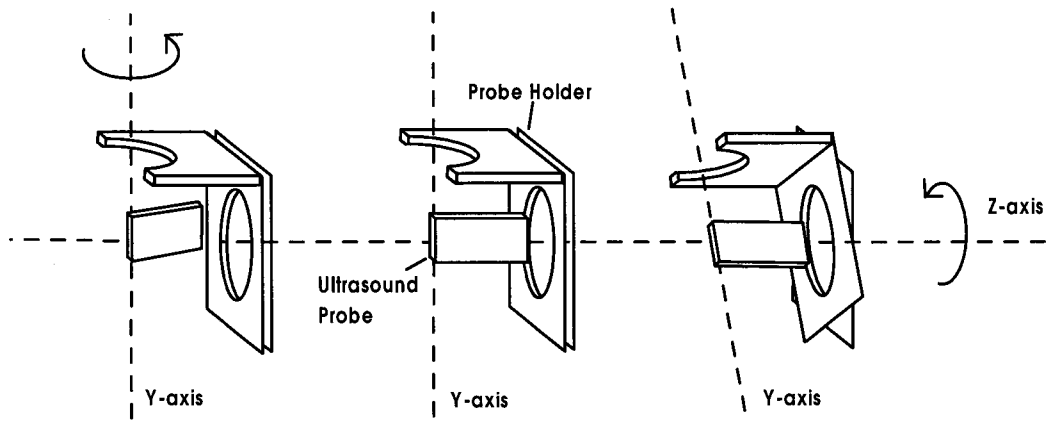

Figure 2-2 The apparatus designed to hold the ultrasound probe and allow the probe to rotate about the transverse plane (y axis) and the frontal plane (z-axis).

One of the difficulties in designing the device was to make the sagittal-frontal axis of rotation (Figure 2-3) at the probe-skin contact point such that the most proximal part of the ultrasound image obtained remained consistent in all 9 rotation trials. This was

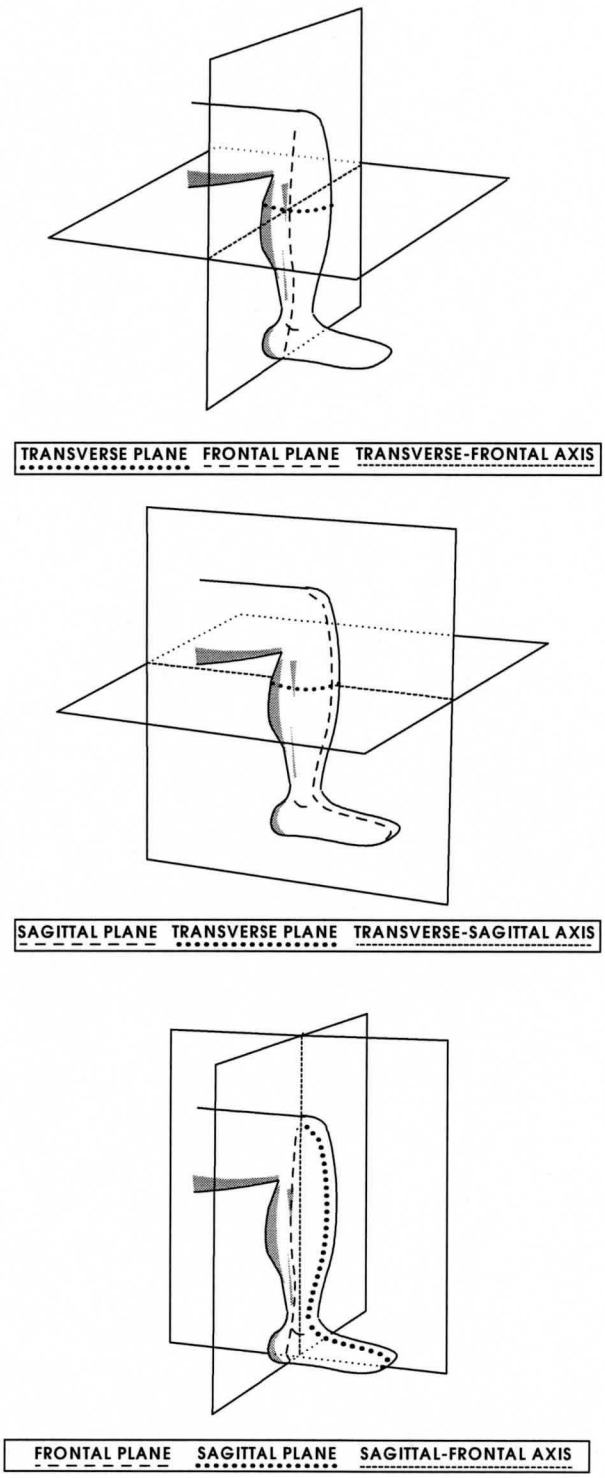

Figure 2-3 An example of the axis of rotation developed from the intersection of two planes

achieved by using one half of a large circular turret (lazy suzan) for the rotation in the transverse plane. This half circle was attached perpendicular to another large circular turret.

From this point forward, rotation in the transverse plane will be referred to as rotation about the y-axis and rotation in the frontal plane will be referred to as rotation about the z-axis. Rotation in the sagittal plane would cause the probe to loose contact with the subject's skin and therefore this rotation was not considered important with regard to the discussion of how probe rotation affects the ultrasound image.

The probe was held in place by a clamp that was attached to a semicircular piece of the turret that traveled in a circular groove. This allowed the probe to pivot about the probe-skin contact point. Each circular piece was fitted with knobs to fix the device to specific y and z rotations. These knobs could be loosened and then retightened to allow for specific rotations. Guidelines were drawn with markings of 5 degree intervals for each axis of rotation. When both rotations were set to their zero position the probe visualized a cross section in the sagittal plane.

2.2.4. Footswitch Synchronization

EMG, torque and angular displacement measurements from the watscope computer were synchronized to images collected by the ultrasound computer via a footswitch signal. Image collection can be initiated on the ultrasound computer by depressing a footswitch. A signal from this footswitch was recorded on the watscope computer. A calibration was done to determine the timing of the footswitch signal relative to images collected by the ultrasound computer. Because of the time resolution

difference between the two devices it was important to determine the timing of the foot switch as it related to image collection. A computer software program was developed to determine if there was any delay between the pressing of the foot switch and the beginning of data collection. The footswitch signal was considered to correspond to the last image collected by the ultrasound computer (frame 169 in the ultrasound movie).

2.3. Experimental Protocol

2.3.1. EMG surface electrode placement

Each subject's skin was prepared for the placement of the surface EMG electrodes. Excess hair was shaved from a one inch square area of skin over the tibialis anterior muscle. The surface electrode for the tibialis anterior was placed on the most proximal part of the muscle just inferior to the tibial tuberosity and lateral to the palpable edge of the tibia. This placement was consistent across all subjects and was necessary because it was the only part of the muscle not covered by the ultrasound probe. Dead skin was removed with a rough pad and any oil was removed from the surface of the skin with an alcohol swab. A ground electrode was placed on the lateral malleolus of the ankle. All of the electrodes were secured to the skin using surgical tape. After the electrodes were attached the subject was asked to place their foot and leg into the boot.

2.3.2. Ultrasound Probe Placement

The ultrasound probe was placed into the probe holding device. The probe was fitted with a Styrofoam stand-off which held the ultrasound transmission gel and also

kept the head of the probe from touching the skin and putting pressure on the muscle, which could affect the measurement. The probe was placed to visualize a central region of the tibialis anterior muscle in a position such that the deep and superficial aponeuroses were clearly visualized throughout contraction. Once the probe was placed and the muscle visualized on the ultrasound monitor, the investigator altered the settings on the ultrasound computer to provide the best image clarity. Then, the investigator rotated the probe in the device until the fascicles were clearly visualized. A built-in depth ruler allowed the investigator to determine changes in MT. Suitability of a chosen probe rotation was further tested by having the subject perform a few zero-load dorsi-flexion contractions. If the image remained clear throughout contraction, that position was taken as the starting position for all ultrasound measurements on that subject.

2.3.3. Testing Protocol

The order of the testing protocol was as follows:

1) The subjects performed a maximum isometric dorsi-flexion contraction at 20° plantar-flexion. This trial was repeated at the end of the experiment to determine the potential effect of fatigue and/or potentiation on EMG activity and force production.
2) The ultrasound probe was placed securely yet comfortably to properly visualize the TA muscle. The subject was asked to perform a slow concentric dorsi-flexion contraction from 20° plantar-flexion to full dorsi-flexion. The subject was instructed to complete the contraction in less than three seconds. The load used

was determined from the original isometric trial and was set to 50% of the Maximum voluntary contraction (MVC).

3) – 10) The next eight trials consisted of the same slow concentric dorsi-flexion contraction with different probe positions. The probe was rotated about either or both the y and z axis in 5° steps for a total of nine different probe positions.

11) The subjects performed a maximum isometric dorsi-flexion contraction at 20° plantar-flexion.

Approximately one minute between trials was required to determine if the data collection was acceptable. The whole protocol lasted for a duration of 45 min to an hour.

2.4. Data Collection

A Watscope data acquisition unit (Northern Digital Inc.) was used to collect the signals from the torque sensor, the potentiometer, the EMG electrodes and the footswitch. The data was sampled at 1000 Hz for a period of five seconds for each trial.
A General Electric™ VingMed System-Five ultrasound machine connected to the 10 MHz linear array probe began data collection at the pressing of a foot switch. The footswitch signal corresponded to the last image collected from a buffer. The machine collected 169 images at 49 .5 frames per second for a total of 3.4 seconds. Thus, each of the three second slow concentric dorsi-flexion trials had 169 temporally stacked images.

2.5. Data Analysis

2.5.1. Data Processing

Custom software was developed using Labview 7 Express™ for calculation and comparison of all of the collected data. The torque sensor data was converted from the computer values to newton metres using the conversion values determined from calibration trials. The signal from the potentiometer was converted from the computer values to degrees using the conversion values determined from calibration trials. The EMG data from the tibialis anterior muscle was converted from the computer values to microvolts and then full-wave rectified. A linear envelope was created by passing the full-wave rectified EMG through a low-pass critically damped filter with a cut off frequency of 3 Hz. The linear envelope was taken to represent the level of muscle activation. This allowed the comparison of EMG from different trials.

The software was designed to use the foot switch signal to synchronize the ultrasound images to the EMG, potentiometer and the torque transducer. The computer analysis of the data began by choosing a joint angle from the potentiometer signal. This joint angle was found in the other eight probe rotation trials. It is important to note that the same angle on different trials related to different times in the collected data. Once this angle was found across all 9 trials, the time value was used within each trial to determine the EMG, torque and frame number corresponding to the joint angle at that time. Therefore, each trial had a different time value for the chosen joint angle and this time value was used to determine the corresponding values of EMG, torque, and image frame number for

that joint angle. These values were saved in a table and the image corresponding to the frame numbers were analyzed for measures of MAP.

2.6. Muscle Architecture Parameter Measurements

2.6.1. Computer Analysis Program

A computer program was developed using Labview 7 Express™ and was designed to measure PA, FL and MT from the manual placement of 6 cursors on the ultrasound image by the investigator. The image analysis program was also developed with an image threshold filter which could be turned off or on and adjusted during the analysis.

2.6.1.1.Image Analysis

The program used the pixel measurements from the image to calculate angles and lengths between specific cursor locations. The area visualized in the image has a known height of 3 cm and the pixel dimensions of the image is 964x721 pixels corresponding to the width and the height of the image respectively (Figure 2-4). Therefore each pixel represented 0.00416 cm. The actual analysis of the image involves placing line segments over specific structures on the muscle image: the superficial aponeurosis, the muscle fascicle and the deep aponeurosis. The image is a sagittal plane cross-section of a tibialis anterior muscle. The top of the image is the skin surface and the bottom of the image visualizes deep into the muscle. At the top of the image is the superficial aponeurosis of the muscle. This is a thick white line. Emerging out of this superficial aponeurosis at an angle are thinner white lines that travel diagonally across the image. These are muscle

fascicles. The fascicles insert at an angle into another thick white line which is the deep aponeurosis.

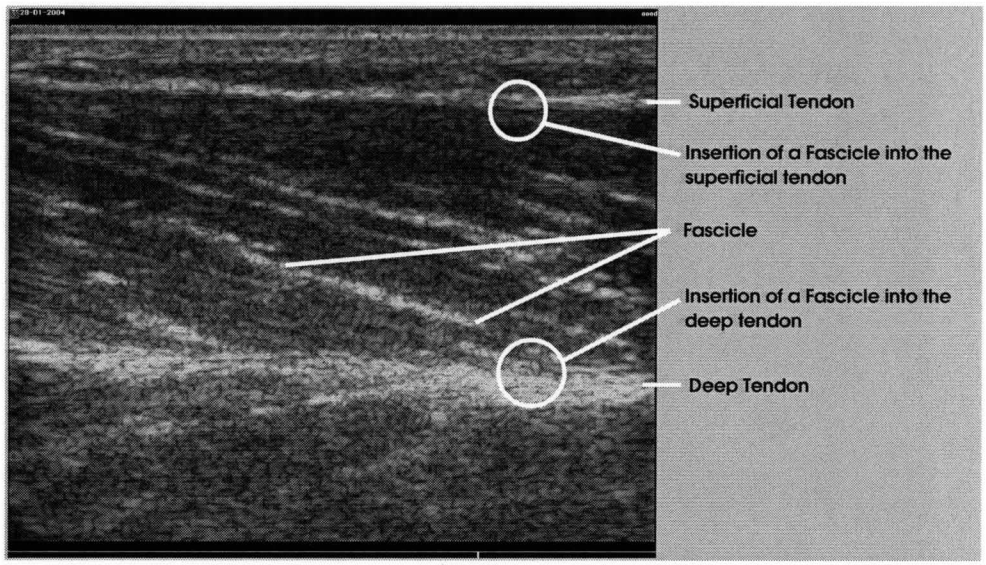

Figure 2-4 The cross-section developed by the ultrasound computer.

Each line segment corresponding to a structure in the muscle was placed by moving two cursors on the image (Figure 2-5). These two cursor positions represented two points on a line. The superficial aponeurosis line is the top line made by placing the top two cursors. The fascicle line is the middle line made by placing the two cursors in the middle of the image. The deep aponeurosis line is the bottom line made by placing the two bottom cursors (Figure 2-5).

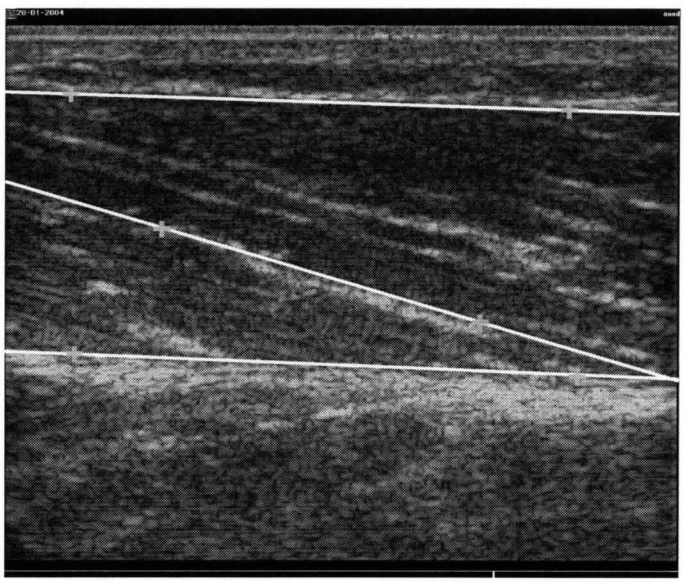

Figure 2-5 The cursor and line locations on the ultrasound image.

The muscle FL was measured as the length of the middle line from its intersection points into both the superficial and the deep aponeurosis. The PA was defined as the average of the angle between the fascicle and the deep aponeurosis and the angle between the fascicle and the superficial aponeurosis. The MT measurement was defined as an average distance of two line lengths. The first line length was measured as the line perpendicular to the deep aponeurosis from the insertion point of the fascicle to the perpendicular lines intersection point into the superficial aponeurosis. The second line length was measured as the line perpendicular to the superficial aponeurosis from the insertion point of the fascicle to the perpendicular lines intersection point into the deep aponeurosis.

2.6.1.2.Image Filtering (Threshold)

The image can be represented in graph form as an array of numbers. The sequence of the numbers corresponds to the location of a pixel in the image. The

magnitude of the number assigned to the pixel is from 0 to 255 and represents the gray shade value that corresponds to that pixel. A gray shade of 0 is black and a gray shade of 255 is white. The Image was altered by taking the array of 256 gray scale values that corresponded to the image and passing the array through a filter before reconstructing the image. The array was filtered by selecting an upper and lower threshold of gray shade values. This meant that any pixel gray shade value below the lower threshold gray shade value would be assigned a value of 0 and return as a black pixel. Any pixel value above the lower threshold value and below the upper threshold value would remain the same. Any pixel value above the upper threshold value would be assigned a value of 255 and return as a white pixel in the image.

2.6.2. Reliability Protocol

A reliability study was performed to determine the inter-class (between subjects) and intra-class (within subjects) variation of muscle architecture parameter measurement using the computer program. This test required four investigators to measure 12 images on four occasions with or without an image filter. This would require the investigators to analyze one image twice for a given trial. Thus the investigator would measure MAP a total of 96 times. The image filter was used to provide distinction between structures in the image and the purpose of the reliability test was twofold. 1. To determine the day to day reliability of muscle architecture measurement. 2. To find the effect of using the image filter to measure MAP.

The inter-class variation would be conducted by averaging the coefficient of variation of each image for all subjects. The intra-class variation would be conducted by

averaging the coefficient of variation of each subject for all images between trails. The coefficient of variation is a measure of the standard deviation of a number of scores divided by the mean value of the scores.

2.7. Statistical Analysis

Comparing the same joint angle for different probe position trials depends on the similarity of the trial. Therefore it was necessary to compare the force at that joint angle as well as the EMG activity to determine if activation would affect the comparison. Therefore a 9(Probe Rotation) X 4 (Joint Angle) Analysis of Variance was performed for each of FL, PA, MT, torque and tibialis anterior EMG. The results from this analysis were used to assess the effect of probe rotation on measures of MAP. Results for torque and EMG were evaluated based on the similarity between trials as a measure of suitability of comparison. Results for the measures of MAP will be compared to the predicted model to determine the effect of probe rotation on measures of MAP.

Chapter 3. Results and Discussion

This section will serve to report and discuss the results of the experiment and has been separated into five parts.

1) The pre and post Maximum Isometric trials.
2) The probe placement and orientation for the slow concentric trials.
3) Legends and information necessary to understand the results from the slow concentric trials.
4) The results of a 4(joint angle) X 9 (probe rotation) analysis of variance for torque and tibialis anterior EMG for the slow concentric trials.
5) Muscle Architecture Parameter results
    i. The results of a reliability study on the measurement of MAP.
    ii. The results of a 4(joint angle) X 9 (probe rotation) analysis of variance for FL, PA and MT.
    iii. The analysis of variance results for FL, MT and PA will be graphed in three dimensions along with the predicted values to illustrate the effect of Y and Z probe rotation on these measures.

3.1. Pre and Post Maximum Isometric Trials

3.1.1. Pre and Post Torque

The average maximum isometric torque collected at 20 degrees plantar-flexion pre-protocol was 43.7 ± 9.8 N.m. The average maximum isometric torque collected at 20

degrees plantar-flexion post-protocol was 43.5 ± 9.4 N.m. Figure 3-1 shows the pre and post measure of maximum isometric torque per subject for the tibialis anterior muscle at 20° plantar-flexion. A single factor ANOVA found no main effect for time in the pre and post measure of torque. This result would suggest that there was no effect of fatigue and/ or potentiation of the muscle caused by the experimental protocol.

3.1.2. Pre and Post Tibialis Anterior Electromyography

The average maximum tibialis anterior EMG collected at 20° plantar-flexion pre-protocol was measured to be 193 ± 95 μV. The average maximum tibialis EMG collected at 20 degrees plantar-flexion post-protocol was 207 ± 113 μV. Figure 3-2 shows the pre and post measure of maximum isometric tibialis anterior EMG per subject at 20° plantar-flexion. A single factor ANOVA showed that there was no main effect for time for measures of EMG per subject. This result illustrates that even though there is great variability between subjects in the measures of EMG the magnitude of the EMG collected during the experiment is consistent from first to last trial showing that fatigue or potentiation would not affect the experiment.

The aspect of interest is the change in force or EMG activity that may reflect a change in MAP. This is not necessarily fatigue or potentiation but could be due to tendon creep or some other unknown mechanism caused by repeated contraction. Because the probe rotation was changed for each trial the same region was not visualized throughout contraction and I must rely on the work of other authors in this area (Kubo et al., 2001; Maganaris et al., 2002).

In their study, Maganaris et al. (1999) found that the coefficient of variation value for repeated scanning of the same area for one subject was found to be less than 8% both at rest and during MVC. This would suggest that the architecture of human muscle remains consistent throughout repeated contractions. Maganaris et al. (2002) conducted a study on how repeated contraction alters the geometry of skeletal muscle. This study showed the greatest change in MAP measurements was after the first of a series of 80% maximum plantar-flexion contractions and this change was associated with tendon creep. This study analyzed the Medial Gastrocnemius muscle and the results may not be comparable to the tibialis anterior muscle. Kubo et al. (2001) studied the effect of repeated contraction on the vastus lateralis muscle and found that changes in elasticity could be related to repeated long duration contractions but not the type of muscle action or the level of force production.

Due to the pre and post measures of torque and EMG and the relatively small load lifted by the participants it is assumed that there was no tendon creep or altering of the geometry of MAP between trials.

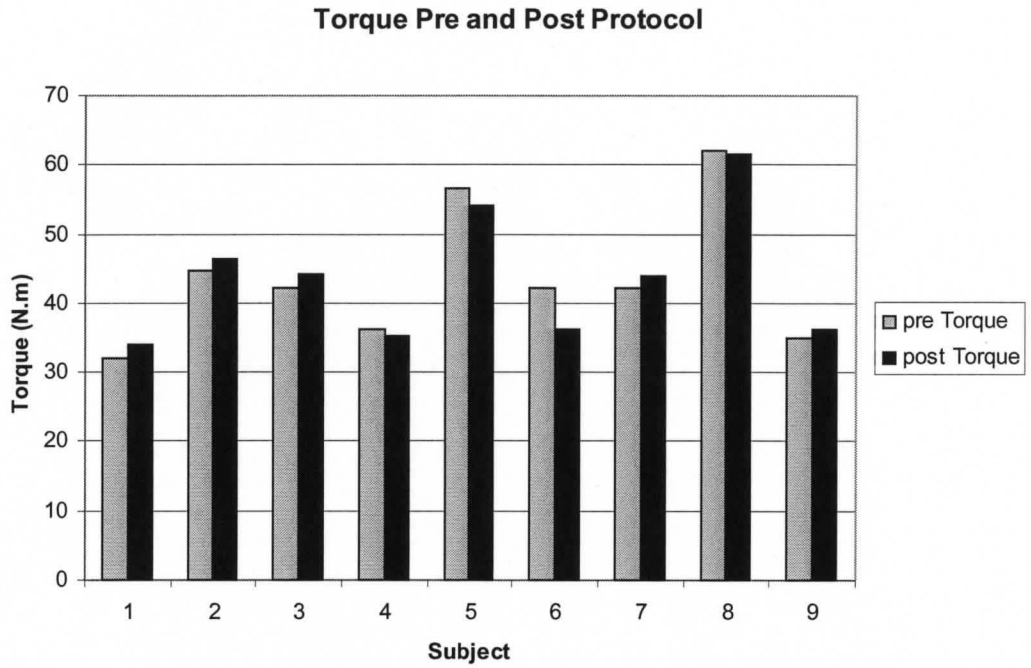

Figure 3-1 Maximum Isometric torque from the tibialis anterior muscle pre and post protocol

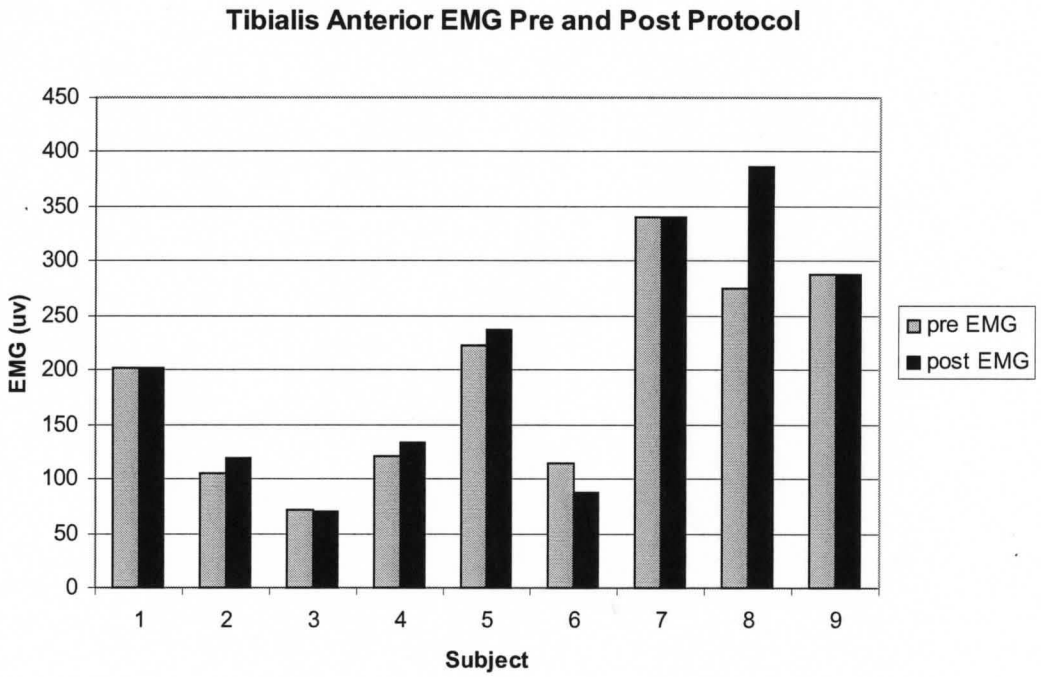

Figure 3-2 Maximum Isometric EMG from the tibialis anterior muscle pre and post protocol.

3.2. Probe Placement and Orientation

3.2.1. Probe Placement

The probe placement chosen for the experiment for all subjects was along the median longitudinal axis of the tibialis anterior muscle which is sometimes defined as a straight line drawn between origin and insertion of the muscle. In the case of the tibialis anterior this line can be drawn parallel to the palpable edge of the tibia (Narici et al., 1996; Hodges et al., 2003). Narici et al. (1996) found that the gastrocnemius muscle architecture could be viewed properly by orienting the transducer along the median longitudinal axis of the muscle. This is consistent to Figure 3-4, showing the original z-rotation of the muscle.

Maganaris et al. (1999) visualized three different regions of the tibialis anterior muscle and found no significant difference between any given characteristic of MAP between the three regions scanned corresponding to a proximal, central, and distal placement. A central region of the muscle was visualized for all subjects.

3.2.2. Probe Orientation

The average original probe orientation for all subjects was recorded to be 14 ± 8 degrees of y-probe rotation and 4 ± 7 degrees of z probe rotation (Figure 3-3).The original probe rotation corresponded to probe rotation 5 for all subjects (Figure 3-5).

A negative degree step in the y probe rotation corresponds to the end of the probe furthest away from the tibialis anterior muscle moving medially with respect to the right leg (Figure 3-3). A negative degree step in the z probe rotation corresponds to the probe rotating clockwise in the frontal plane (Figure 3-3).

Reeves et al. (2003) described the proper probe position as perpendicular to the dermal surface along the mid-sagittal plane of the TA muscle at the site corresponding to the thickest portion of the muscle. Hodges et al. (2003) adjusted the angle of the transducer obliquely to the sagittal plane of the lower leg to image the tibia deep to the muscle. In the study by Hodges et al. (2003) the position of the transducer was adjusted to visualize optimally the muscle fascicles and the intramuscular tendon that runs down the centre of the muscle. These probe orientation conditions are consistent with the range of values of original y-probe rotation found in the present study (Figure 3-3).

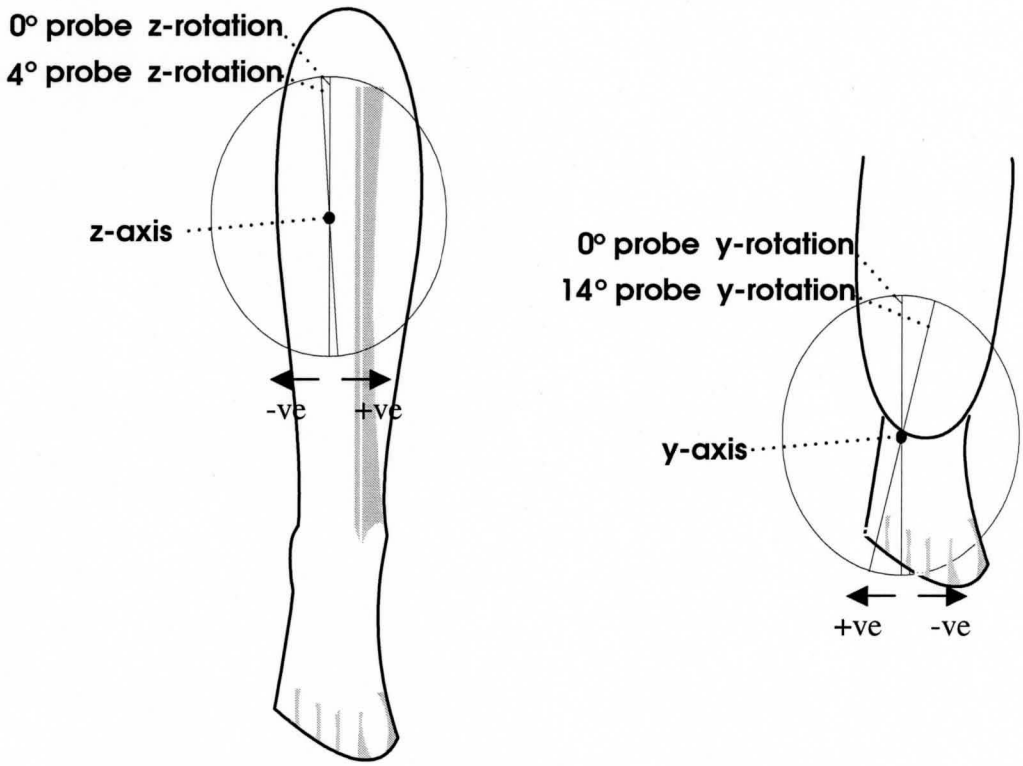

Figure 3-3 Original Z and Y Probe rotation for all Subjects

3.2.3. Proper Plane of Contraction

The proper plane of contraction is determined by researchers as the plane containing the line of action of the most clearly visualized fascicle. It is difficult from ultrasound to distinguish whether the structures visualized are continuations of the same fascicle or regions of connection between two fascicles. It is also difficult to determine if fascicles remain in the plane of visualization of an ultrasound probe. The importance of this plane of contraction for research is to ensure that the same fascicle is visualized throughout contraction and that the fascicle's movement can be defined in 2-dimensions without consideration of the fascicle rotating out of the plane of visualization.

Kawakami et al. (1998) stated; *By visualizing the fascicles along their lengths from the superficial to the deep aponeurosis one can be convinced that the plane of the ultrasonogram is parallel to the fascicles, otherwise the fascicle length would be overestimated and the fascicle angle would be underestimated.* Hodges et al. (2003) concluded that maintenance of an optimal image ensured constant orientation with respect to the muscle fascicles. Reeves et al. (2003) attempted to scan the muscle along the sagittal plane of the fascicles so that in each image the entire visible length of the fascicles could be tracked. Such an investigation is beyond the scope of this experiment as it requires a thorough 3 dimensional analysis of the structure and action of individual muscle fascicles. This study attempts to determine a standardized method of probe orientation to reduce errors in MAP measurements due to improper probe orientation.

3.3. Slow Concentric Trials Legends and Information

3.3.1. Joint Angle

Throughout this section the joint angles chosen for the experiment will be represented as joint angle 1, 2, 3, and 4. These joint angles correspond to angles achieved by the subjects in the slow concentric dorsi-flexion trials and proceed sequentially from plantar-flexion to dorsi-flexion. Table 3-1 will act as a legend to show the actual angles used. The angles were chosen as the smallest and greatest angle achieved by all subjects.

Joint Angle	True angle (degrees)	Plantar/Dorsi Flexion
1	16.7	Plantar
2	8.8	Plantar
3	0.9	Plantar
4	7.0	Dorsi

Table 3-1 Joint angle legend

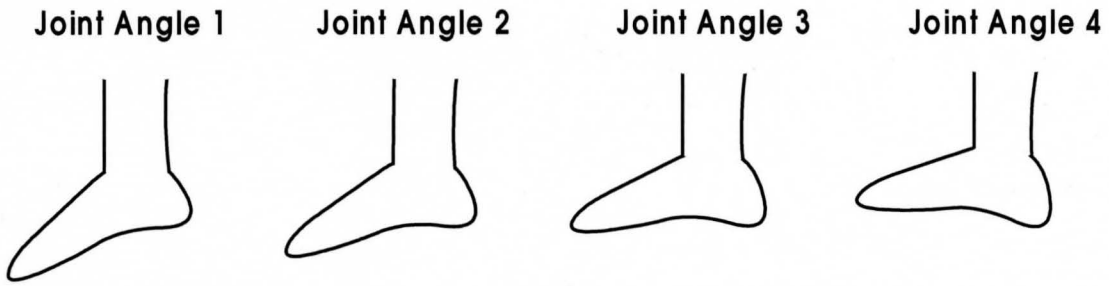

Figure 3-4 Representation of the Joint angles used in the experiment

3.3.2. Time for Slow Concentric Contractions

Table 3-2 shows the total time ± standard deviation required for the contractions from joint angle 1 to 4 for all subjects.

Subject	Time (ms)	Standard deviation
1	838	97
2	787	102
3	960	097
4	641	169
5	625	219
6	771	092
7	596	093
8	494	041
9	565	062
Average	697	150

Table 3-2 Mean time for each subject to complete the slow concentric contraction

Reeves et al. (2003) concluded that a constant fibre length cannot be assumed from the same joint angle during concentric contractions of different angular velocities. Table 3-2 illustrates that the time for completion of each trial was consistent within subjects. Due to the small standard deviation in time to completion for each subject it is assumed that the angular velocities achieved by the participants were consistent between trials and this would not add to the variability in the measurements.

3.3.3. Statistical Graphs

The graphs for each measure are the means ± standard error (error bars) from the results of a 4 (joint angle) X 9 (probe rotation) repeated measures analysis of variance based on 9 subjects. Three graphs are presented for each measure. These graphs represent the main effects for joint angle, probe rotation as well as the interaction between joint angle and probe rotation on each measure. The analysis of variance summary table can be seen in Appendix A for each measure. The results for each measure will be explained with respect to the summary table and the results of a Tukey honestly significant difference post hoc analysis to determine differences between means.

3.3.4. Two-dimensional and Three-dimensional graphs

The graphs for the main effect of probe rotation from a 4 (joint angle) X 9 (probe rotation) analysis of variance for the measures of torque, tibialis EMG, FL, PA, and MT are presented as two-dimensional plots. The numbers corresponding to probe rotation cannot be read from left to right as a sequence of events. Each value from 1 to 9

represents a combination of both y and z probe rotation. Figure 3-5 outlines how these values from 1 to 9 correspond to the rotation of the probe. The ANOVA graphs are displayed as a two-dimensional plot for simplicity; however, it is important to note how the numbers relate to each other in space, i.e., 3 is not next to 4.

a.

Probe Rotation	y rotation (degrees)	z rotation (degrees)
1	-5	-5
2	0	-5
3	5	-5
4	-5	0
5	0	0
6	5	0
7	-5	5
8	0	5
9	5	5

b.

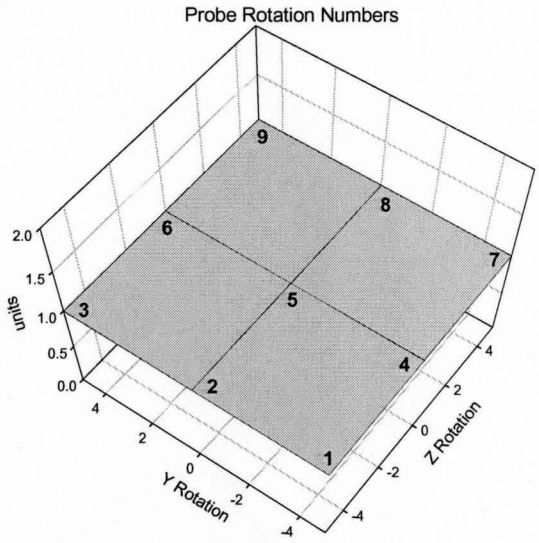

Figure 3-5 Probe rotation legend (a) and 3-D graph legend (b).

3.4. Torque and Tibialis anterior EMG (slow concentric trials)

The measures of torque and EMG that correspond to the images analyzed for MAP for the chosen joint angles are presented below. These measures were used to determine the similarity between trials in order that a comparison of MAP between probe rotations could be performed.

3.4.1. Torque

The average torque measurements for all subjects at each joint angle ± Standard Error are shown in Table 3-3 and also graphed in Figure 3-6 a.

Joint Angle	Mean Torque(N.m)	St_Err (N.m)
1	20.4	2.1
2	19.7	1.6
3	21.1	1.5
4	22.6	1.8

Table 3-3 Mean Torque ± SE for all subjects at each joint angle.

The results of the 4 (joint angle) X 9 (probe rotation) repeated measures ANOVA showed a main effect for joint angle at a p-value of < 0.01 with no main effect for probe rotation and no significant interaction. A Tukey HSD post hoc was performed for joint angle and revealed a critical value of 1.59 N.m. This shows that the significant difference between means can be seen between Joint Angles 1 and 4 and 2 and 4. This result indicates that each probe rotation shows the same relative effect for joint angle with no statistically significant difference in the absolute magnitude of the measurements between probe rotations (Figure 3-6. b and c)

Torque was a measure used to validate that each of the nine slow concentric contractions for each subject were similar. The eventual analysis of MAP requires that each contraction be as identical as possible. However, Kaya et al. (2002) concluded that the relationship between FL and muscle force is complex and highly non-linear.

Therefore, even though the torque values were similar between contractions one cannot conclude from these values alone that the muscle's structural behaviour is consistent between trials. It is, however, acceptable to assume that the degree of experimental control sufficient to analyze MAP, based on an analysis of torque, was achieved.

a.

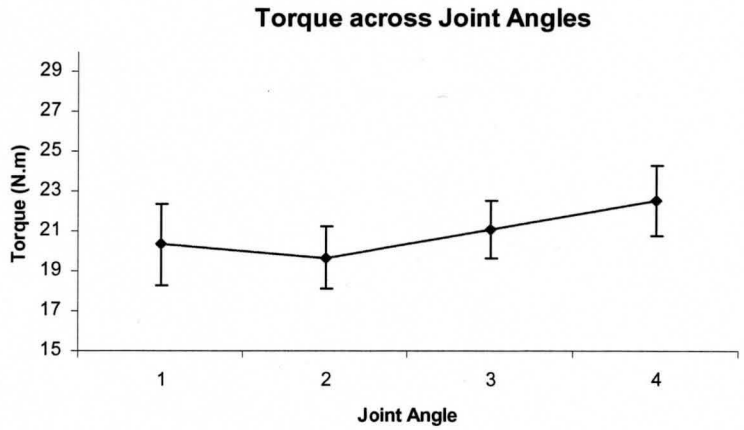

b.

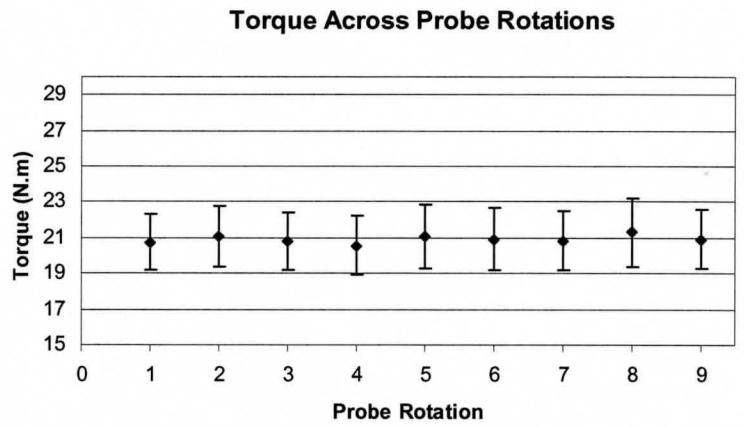

c.

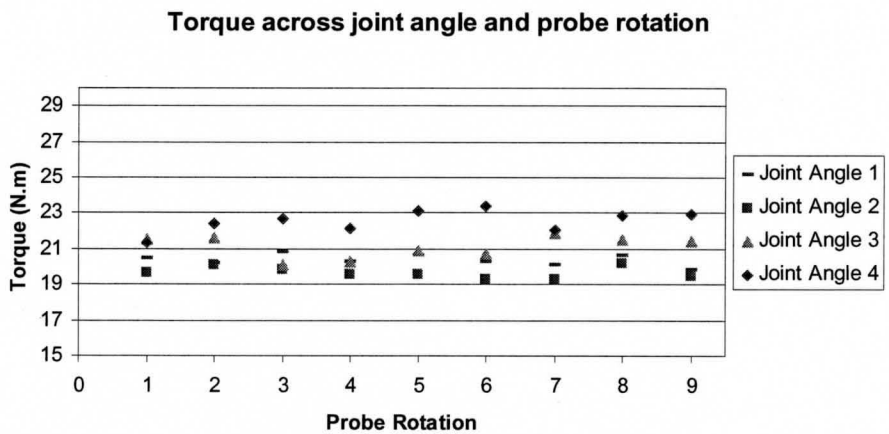

Figure 3-6 The results from a 4(joint angle) X 9 (probe rotation) analysis of variance for measures of Torque. The graphs are the Means ± SE Graphed by : a) Joint Angle b) Probe Rotation c) Joint Angle/ Probe Rotation interaction

3.4.2. Tibialis Anterior Electromyography

The average tibialis anterior EMG measurements for all subjects at each joint angle ± Standard Error are shown in Table 3-4 and also graphed in Figure 3-7 a.

Joint Angle	Mean EMG(μV)	St_Err (μV)
1	90.9	15.8
2	99.1	17.7
3	127.7	21.6
4	160.7	24.4

Table 3-4 Mean Tibialis anterior EMG ± SE for all subjects at each joint angle.

The results of the 4 (joint angle) X 9 (probe rotation) repeated measures ANOVA showed a main effect for joint angle at a p-value of < 0.01 with no main effect for probe rotation and no significant interaction. A Tukey HSD post hoc was performed for joint angle and revealed a critical value of 25.5 μV. This shows that a significant difference between means can be seen between joint angles 1 and 3, 1 and 4, 2 and 3, 2 and 4, and 3 and 4. This result indicates that each probe rotation shows the same relative effect for joint angle with no statistically significant difference in the absolute magnitude of the measurements between probe rotations (Figure 3-7. b and c)

a.

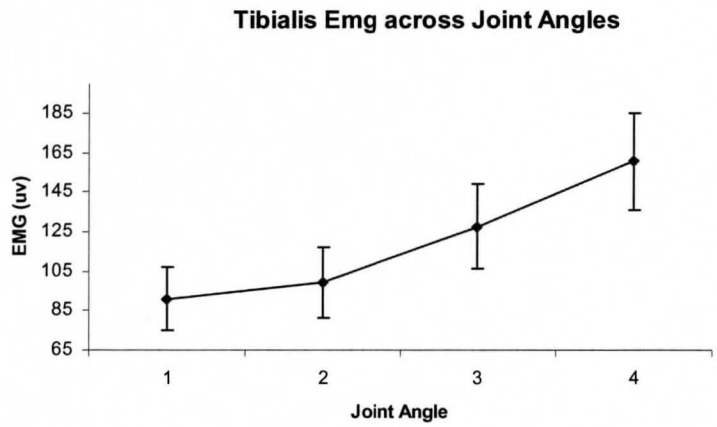

b.

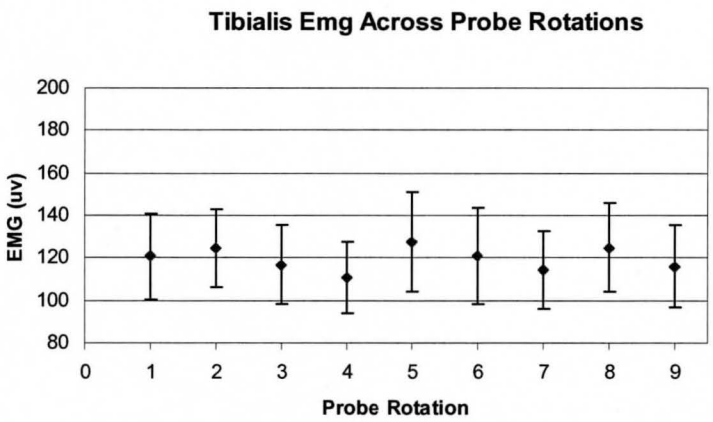

c.

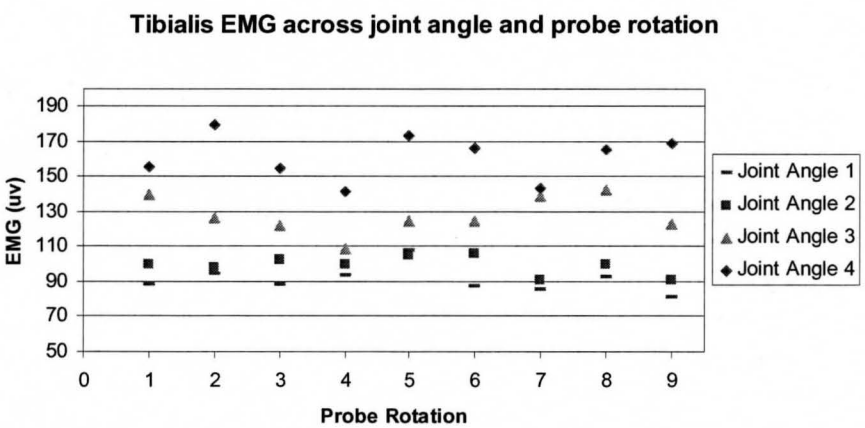

Figure 3-7 The results from a 4(joint angle) X 9 (probe rotation) analysis of variance for measures of Tibialis anterior EMG. The graphs are the Means ± SE Graphed by : a) Joint Angle b) Probe Rotation c) Joint Angle/ Probe Rotation interaction

Reeves et al. (2003) found no significant difference in the EMG activity of tibialis anterior for different angular velocities for either concentric or eccentric contractions. Hodges et al. (2003) observed that ultrasound imaging can be used to detect low levels of muscle activity, as measured by EMG, but cannot discriminate between moderate and strong contractions. For the tibialis anterior Hodges et al. (2003) found that PA could reliably detect a change in EMG of 9% while FL and MT could predict a change in EMG of 16%. The greatest difference noticed in the current study for EMG between probe rotations 4 and 5 is approximately 15% which would illustrate that the values obtained in the current investigation could cause values of MAP not consistent to an identical contraction. However, the values of EMG obtained are not statistically significant for probe rotation. This would suggest that the contractions are identical. Due to the fact that MAP are not very sensitive to measures of torque and EMG, it is concluded that the contractions are similar with respect to torque and EMG but this does not necessarily indicate that the measures of MAP are comparable across probe rotation.

3.5. Muscle Architecture Parameter Results

3.5.1. Reliability Study

The results of this reliability study are discussed as coefficients of variation. A coefficient of variation is a measure of the standard deviation of a group of numbers divided by the mean of the group. This measure will be used to determine the relative degree of reliability of the measurements of MAP both within and between investigators.

The Reliability study will also assess the technique used to measure the images as there was both a filtered and a non-filtered condition for each investigator for each trial.

MAP		non filtered	non filtered	non filtered	filtered	filtered	Filtered
		mean	standard deviation	CofV (%)	mean	standard deviation	CofV (%)
Fascicle length	within subjects	7.1 cm	0.5 cm	7.2	6.9 cm	0.5 cm	7.6
	between subjects		0.6 cm	8.3		0.6 cm	8.7
Pennation angle	within subjects	12.3 deg	0.8 deg	6.8	12.6 deg	0.9 deg	7
	between subjects		1.0 deg	8.3		1.1 deg	8.7
Muscle thickness	within subjects	1.46 cm	0.03 cm	1.8	1.45 cm	0.03 cm	1.7
	between subjects		0.03 cm	2		0.03 cm	1.9

Table 3-5 Reliability study table reporting mean, standard deviation and coefficient of variation for filtered and non-filtered analysis of MAP.

Table 3-5 presents the results of a reliability study in values of mean, standard deviation and coefficient of variation for measures of FL, PA and MT in both a filtered (threshold) and a non-filtered condition. The results show that there is no difference between the filtered and non-filtered condition for reliability of measurement.

Narici et al. (1996) found coefficients of variation of 4.8% for MT, 9.8% for PA and 5.9% for FL for repeated measurement of ultrasound images. Maganaris et al. (1999) found that the coefficient of variation value for repeated analysis of a given scan of tibialis anterior was less than 3% for any given characteristic of MAP at rest and during MVC. These values are comparable to the values obtained in the current investigation. The magnitude of the coefficient of variation for measures of FL and PA found in the

literature and the current investigation could affect the comparison of MAP across probe rotations as these values present a potential error in measurement. However, the relatively small coefficient of variation and standard deviation observed for MT shows that this is a highly reliable measure.

3.5.2. Fascicle Length

The average fascicle length (FL) measurements for all subjects at each joint angle ± Standard Error are shown in Table 3-6 and also graphed in Figure 3-8 a.

Joint Angle	Mean FL(mm)	St_Err (mm)
1	74.0	4.4
2	64.6	3.4
3	58.4	2.9
4	52.1	3.0

Table 3-6 Mean FL ± SE for all subjects at each joint angle.

The average FL measurements for all subjects at each probe rotation ± Standard Error are shown in Table 3-7 and also graphed in Figure 3-8 b.

Probe Rotation	Mean FL (mm)	St_Err (mm)
1	67.7	4.5
2	66.2	4.4
3	61.5	3.2
4	62.9	3.4
5	64.2	4.6
6	57.4	3.1
7	61.8	4.5
8	59.9	3.6
9	59.2	2.9

Table 3-7 Mean FL ± SE for all subjects at each probe rotation.

The results of the 4 (joint angle) X 9 (probe rotation) repeated measures ANOVA showed a main effect for joint angle at a p-value of < 0.01 and a main effect for probe rotation at a p-value of < 0.05 with no significant interaction. A Tukey HSD post hoc was performed for joint angle and revealed a critical value of 3.89 mm. This shows that the significant difference between means can be seen between all four joint angles. The Tukey HSD analysis for the main effect for probe rotation yielded a result of 9.19 mm. This value shows that there is a significant difference between PR1 and PR6 as can be seen from Figure 3-8 b. This result indicates that each probe rotation shows the same relative effect for joint angle yet there is a statistically significant difference in the absolute value of some of the measurements due to probe rotation (Figure 3-8 c).

The joint angle effect noticed for FL is an expected result of contraction and the resulting dorsi-flexion of the ankle (McComas, 1996). The fascicle shortening is expected to be directly linked to the summation of the shortening of many sarcomeres in series to create tension and cause movement (McComas, 1996). This is a similar result to that noticed in the literature regarding the tibialis anterior (Maganaris et al., 1998; Reeves et al., 2003; Hodges et al., 2003). The range of values for tibialis anterior FL at rest and at MVC from Maganaris et al. (1999) for the superficial bi-pennate part of the muscle ranged from 8.9 ± 0.4 cm to 6.6 ± 0.4 cm at rest and 5.5 ± 0.4 cm to 4.0 ± 0.3 cm at MVC for ankle angles corresponding to 30° plantar-flexion and 15° dorsi-flexion respectively at a central scanning region. These values seem to correspond well to the values obtained in the present study considering the 45% load lifted and the ankle angles achieved during

the experiment. The ranges of values observed in the current study are from 7.4 ± 0.4 cm to 5.2 ± 0.3 cm.

Each probe rotation showed the same relative effect for joint angle. This would suggest that the probe rotations used in this study all provide acceptable MAP results for studies that require relative changes during contraction (Kawakami et al., 2002; Maganaris et al., 1999). However, the magnitude of FL difference noticed in the present study to be 18% between probe rotation 1 and 6 could substantially affect studies that require absolute lengths. Wickiewicz et al. (1984) used the length of fascicles to determine the number of sarcomeres in series and the force-velocity characteristics of muscle. Aagaard et al. (2001) used physiological cross-sectional area as a measure of the force producing capability of a muscle. This measure requires an absolute value of fascicle length.

a.

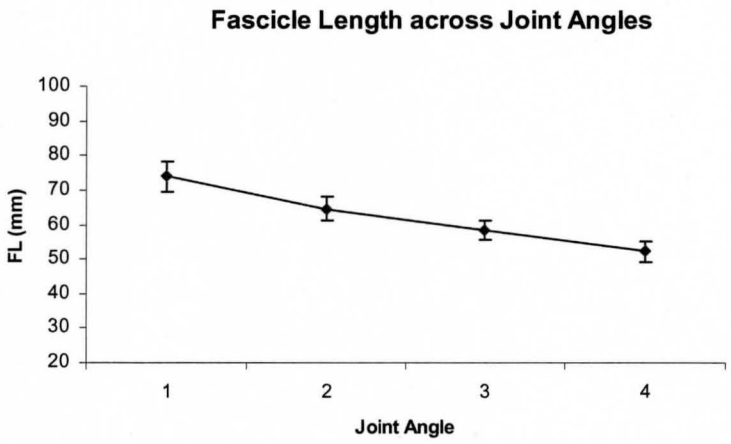

b.

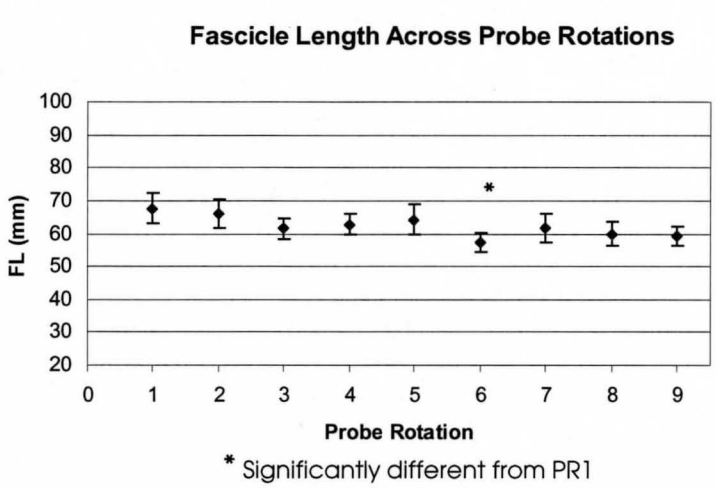

c.

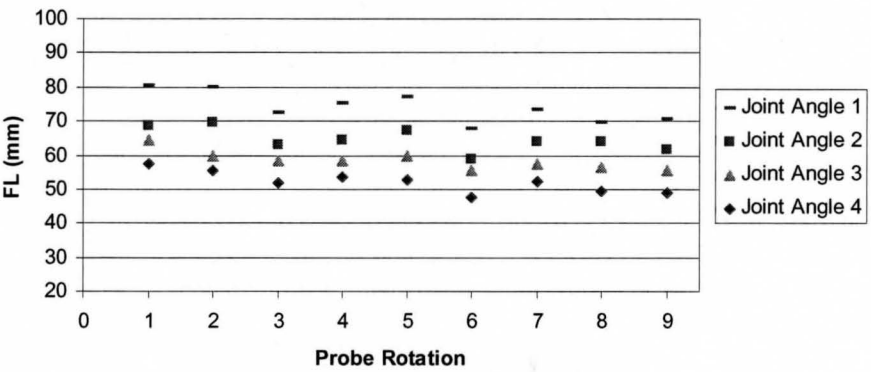

Figure 3-8 The results from a 4(joint angle) X 9 (probe rotation) analysis of variance for measures of fascicle length. The graphs are the Means ± SE Graphed by: a) Joint Angle b) Probe Rotation c) Joint Angle/ Probe Rotation interaction

The straight line approximation of the FL used in this study is accepted in planimetric models used by Maganaris et al. (1999). However, the determination of FL as the length of the line intersecting the deep and superficial aponeurosis as used in the analysis program may have overestimated the actual length of the fascicle. The insertion points of the fascicles were not visualized on the ultrasound image because of the size of the viewing window. Therefore the analysis program would interpolate the insertion points as the intersection points of a straight line drawn along the visualized fascicle into the deep and superficial aponeurosis. However, Reeves et al. (2003) used a similar technique to estimate the length of the fascicle. To determine the error that could be associated with this technique, Reeves et al. (2003) moved the ultrasound probe along the mid-sagittal plane of the muscle and measured the full length of a fascicle. The actual FL was compared to the estimated FL and the order of error associated with the estimated method was 2.4%

3.5.3. Pennation Angle

The average pennation angle (PA) measurements for all subjects at each joint angle ± Standard Error are shown in Table 3-8 and also graphed in Figure 3-9 a.

Joint Angle	Mean PA(degrees)	St_Err (degrees)
1	12.0	0.8
2	13.6	0.8
3	15.0	0.8
4	16.9	0.8

Table 3-8 Mean Pennation Angle ± SE for all subjects at each joint angle.

The results of the 4 (joint angle) X 9 (probe rotation) repeated measures ANOVA showed a main effect for joint angle at a p-value of < 0.01 with no main effect for probe rotation and no significant interaction. A Tukey HSD post hoc was performed for joint angle and revealed a critical value of 0.639 degrees. This shows that the significant difference between means can be seen between all four joint angles. This result indicates that each probe rotation shows the same relative effect for joint angle with no statistically significant difference in the absolute magnitude of the measurements between probe rotations (Figure 3-9 c).

The joint angle effect noticed in the study is another expected result of muscular contraction in a pennate muscle (McComas, 1996). As a fascicle shortens during contraction, it causes displacement of the intramuscular tendon (deep aponeurosis) in the direction of the line of action of the muscle and brings the points of insertion of the fascicle closer together (McComas, 1996). This results in a change in the PA. The range of values for tibialis anterior PA in Maganaris et al. (1999) for the superficial bi-pennate part of the muscle ranged from 9.5 ± 1.7 degrees to 13.2 ± 1.7 degrees at rest and 15.4 ± 3.1 degrees to 22.1 ± 4.7 degrees at MVC for ankle angles corresponding to 30 degrees plantar-flexion and 15 degrees dorsi-flexion respectively at a central scanning region. The values achieved in the current study range from 12.0 ± 0.8 degrees to 16.8 ± 0.8 degrees.

The greatest difference noticed between probe rotations for the current study is from 13.6 ± 1.0 deg to 15.5 ± 0.8 deg or a 12% difference corresponding to probe rotations 5 and 1 respectively. Kawakami et al. (1995) noticed an increase in fibre PA from 16.5 to 21.3 degrees or 29% in the triceps brachii muscle following training.

Aagaard et al. (2001) noticed an increase in PA from 8.0 ± 0.4 degrees to 10.7 ± 0.6 degrees or 33% in the vastus lateralis muscle following training. It is unlikely that Kawakami et al. (1995) or Aagaard et al. (2001) chose probe orientations that were substantially different pre to post training. However, probe orientation could be a potential cause of error in their measurement of PA and this could affect the interpretation of their results.

a.

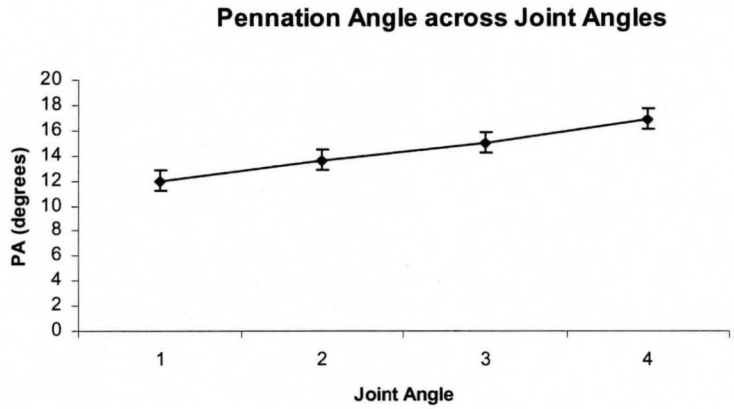

b.

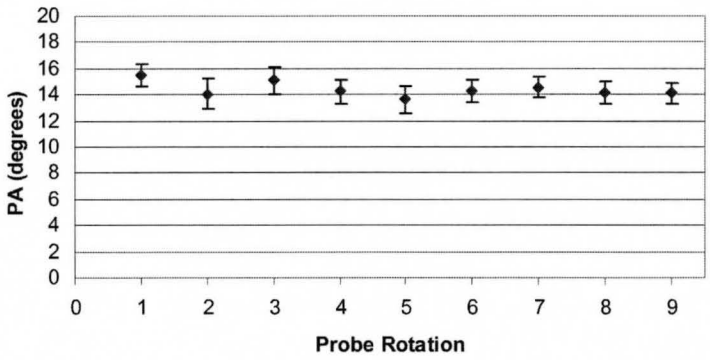

c.

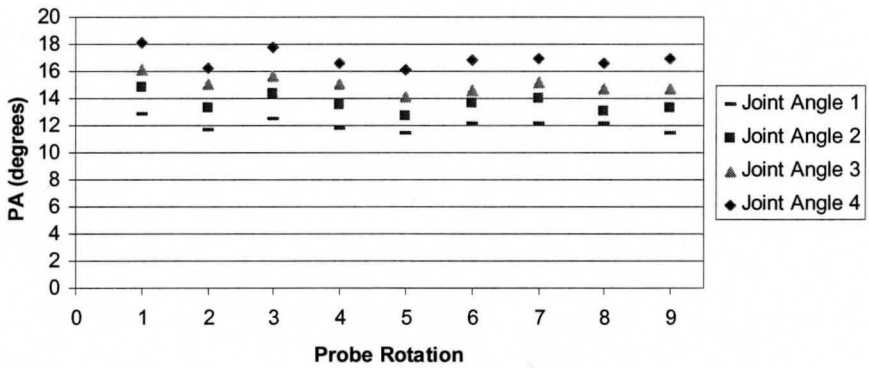

Figure 3-9 The results from a 4(joint angle) X 9 (probe rotation) analysis of variance for measures of Pennation Angle. The graphs are the Means ± SE Graphed by : a) Joint Angle b) Probe Rotation c) Joint Angle/ Probe Rotation interaction

3.5.4. Muscle Thickness

The average muscle thickness (MT) measurements for all subjects at each probe rotation ± Standard Error are shown in Table 3-9 and also graphed in Figure 3-10 b.

Probe Rotation	Mean MT(mm)	St_Err (mm)
1	17.2	1.0
2	15.3	1.2
3	15.6	1.0
4	15.2	1.3
5	14.2	0.9
6	13.7	0.9
7	15.0	1.2
8	14.2	1.1
9	13.8	1.0

Table 3-9 Mean Muscle Thickness ± SE for all subjects at each joint angle.

The results of the 4 (joint angle) X 9 (probe rotation) repeated measures ANOVA showed a main effect for probe rotation at a p-value of < 0.01 with no main effect for joint angle and no significant interaction. The Tukey HSD analysis for the main effect for probe rotation yielded a critical value of 2.09 mm. This value shows that there is a significant difference between PR1 and PR5 through PR9 as can be seen from Figure 3-10 b. This result indicates that each probe rotation shows an absolute difference in the magnitude of MT measurements (Figure 3-10 b and c).

a.

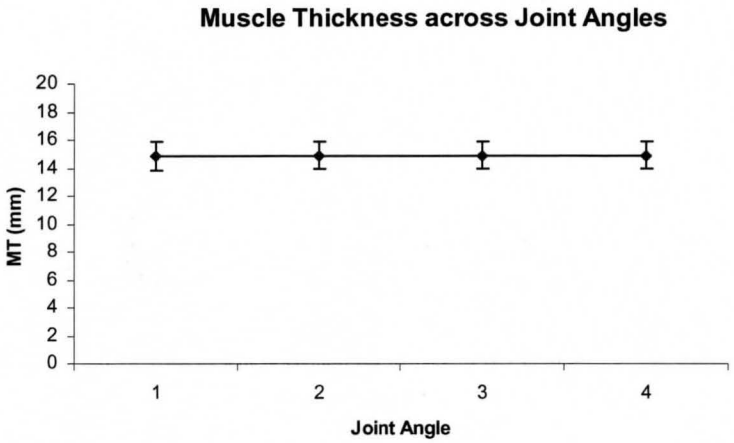

b.

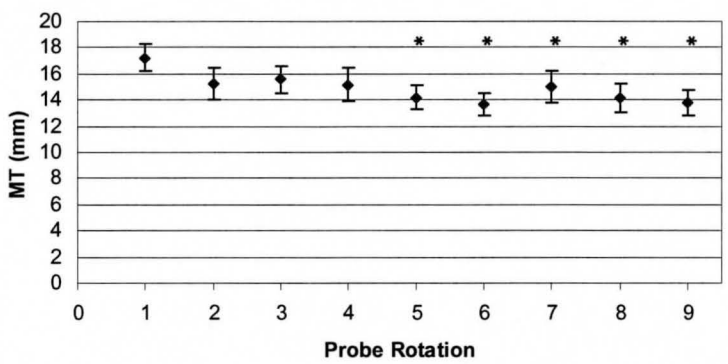

*Significantly different from PR1

c.

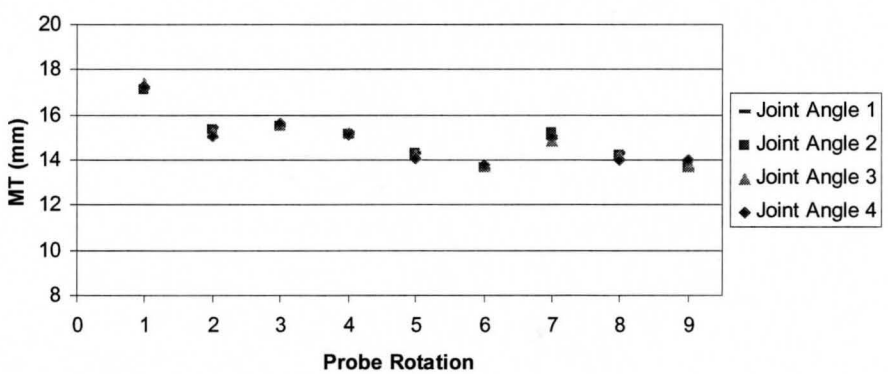

Figure 3-10 The results from a 4(joint angle) X 9 (probe rotation) analysis of variance for measures of muscle thickness. The graphs are the Means ± SE Graphed by:a) Joint Angle b) Probe Rotation c) Joint Angle/ Probe Rotation interaction

The MT measured by Maganaris et al. (1999) was found to remain constant regardless of ankle angle, type, or level of contraction. The value reported was 1.5 ± 0.3 cm. The constant MT has been observed by other authors and has been used to develop planimetric muscle models that use changes in PAs and assumes straight muscle fibres to predict changes in muscle length (Maganaris et al., 1999).

The constant thickness noticed in Maganaris et al. (1999) corresponds to observations of Narici et al. (1996) but contrasts those of Herbert and Gandevia (1995) who found substantial increases in the thickness of the human brachialis muscle during elbow flexion from MVC to rest. Reeves et al. (2003) also noticed changes in tibialis MT during shortening and lengthening contractions. They found that the distance between aponeuroses at a constant ankle angle was significantly greater during eccentric versus concentric contractions and attributed this difference to the smaller PAs and greater FLs noticed in a concentric motion (Reeves et al., 2003). Reeves et al. (2003) also proposed a mechanism of increased MT due to increased compliance in the SEC from an eccentric action.

Hodges et al. (2003) found changes in MT of tibialis anterior. However, this may be due to the proximal site visualized in their study. Hodges et al. (2003) placed the ultrasound probe just inferior to the tibial tuberosity and in parallel to the palpable edge of the tibia. This is the most proximal portion of the muscle where the deep aponeurosis ends and the fascicles converge.

The scanned region of the tibialis anterior chosen for this experiment as well as that of Maganaris et al. (1999) is an area just lateral to the palpable edge of the tibia

where there is no detectable increase in the thickness of the muscle. This is not the only region where MAP can be visualized and the choice of probe placement may affect the measures of MAP that an experimenter observes (Maganaris et al., 1999; Hodges et al., 2003; Reeves et al., 2003).

Gans and Bock (1965) noticed that *thickening of pennately arranged fibres is compensated for by the change in fibre angle during contraction; thus surfaces of origin and insertion remain parallel and equidistant* (Reeves et al., 2003). This theory proposes a possible mechanism for changes in FL and PA without changes in MT. It also presents the question as to whether changes in MAP can validate the constant volume maintained by muscle throughout contraction. I believe that in order to determine the relationship between volume and MAP we need to consider the 3 dimensional changes in muscle during contraction. Due to the fact that MAP measurements only provide a two dimensional representation of muscle behaviour, MAP measurements from ultrasound may not be a good indicator of muscle volume. Also, there may be a thickening of the muscle in an area not visualized by the ultrasound image. I believe this can be shown to be true upon external analysis of a contraction of one's tibialis anterior muscle. It is clear upon visual or manual observation that the part of tibialis anterior muscle just inferior to the tibial tuberosity and in parallel to the palpable edge of the tibia seems to increase in thickness upon contraction. This is the area visualized in Hodges et al. (2003) where a change in MT is observed (Figure 3-11). The central region of the tibialis muscle shows no clear observable increase in thickness during contraction. This is the region visualized

in the present study as well as the study performed by Maganaris et al. (1999)(Figure 3-11). This is the area that corresponds to the average probe orientation.

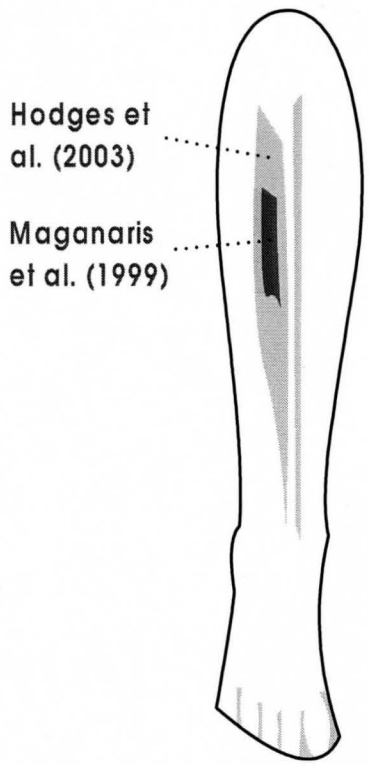

Figure 3-11 The probe placement used in this study (dark grey)

The constant MT throughout the joint movement facilitates the comparison of probe rotation effects on measures of MT. This becomes quite evident from the analysis of variance results. MT appears to be the most suitable measure to determine the effect of probe rotation on measures of MAP. The constant MT, coupled with the high reliability of the measurement technique, encourages the belief that these results are highly reproducible. The result of this finding would be to advise researchers to determine the proper probe placement through a measurement of the MT. However, the use of MT to determine the proper probe placement depends on two important assumptions: 1) that the

muscle structure is similar to the predicted figures and equations, and 2) investigators would be able to determine changes in MT from manual observation. However, Kawakami et al. (1998) noticed that the echoes from interspaces of the fascicles were sometimes imaged more clearly along the length of the fascicles when the plane of the ultrasonogram was changed slightly diagonally to the longitudinal line of each muscle. Also, Reeves et al. (2003) noticed that the TA muscle does not act solely in a sagittal plane and this may result in scanning the muscle from a slightly different orientation, resulting in the appearance of an increased distance between aponeuroses. These findings would suggest that the proper plane of contraction can not be located by measures of MT alone.

3.5.5. MAP graphed in Three-dimension by Probe Rotation

The muscle architecture parameter results are graphed by probe rotation to illustrate the relative effect of both y and z probe rotation on each measure. The means graphed are those taken from Figure 3-8 b, 3-9 b and 3-10 b respectively.

3.5.5.1.Actual versus predicted differences

The smallest mean value of each parameter taken from the ANOVA graph for the main effect of probe rotation was used to determine the predicted change in MAP due to a rotation of the ultrasound probe in the transverse and frontal plane. These predicted values were then graphed 1) independently, to show the trend or shape of the graph

caused by probe rotation and 2) combined with the actual mean values to show the difference in the magnitude of the observed versus predicted values.

A comparison of the shape of the predicted graph to a graph of the observed values could indicate whether the equations developed could be used to predict the structure of the muscle in three dimensions. The equations were developed to coincide with observations made by researchers regarding their choice of probe orientation (Kawakami et al., 1998; Reeves et al., 2003; Hodges et al., 2003).

The absolute magnitude of the measured values of FL, PA and MT are different between probe rotations (Figures 3-12, 3-15, and 3-18). In order to standardize these values a strict adherence to specific guidelines of probe placement and orientation could help to generalize results from other studies to be used in muscle models. (Maganaris et al., 1999; Wickiewicz et al., 1984)

The measures of FL and PA do not follow the trend of the predicted values and have differences in magnitude greater than predicted (Figures 3-14, 3-17, and 3-20). Therefore, the muscle may not be able to be treated like a rectangular prism. Another possible reason for the difference could be due to the error associated with the measurement technique which may not allow for this type of comparison. If the muscle structure cannot be treated like a rectangular prism and/or the measurement technique is not accurate then it may not be feasible to believe that an individual investigator would be able to determine the proper plane of contraction from manual measurements of MAP. Therefore, it is difficult to ascertain whether an investigator could be certain that the plane of visualization and the plane of contraction are consistent. The adherence to

certain guidelines may be the only tool available to define the correct visualization position.

The observed MT values have a difference in magnitude and trend to the predicted values. The equation dictates that there should be no effect of z rotation on this measure. However, a z rotation could cause the deep aponeurosis and the superficial aponeurosis to no longer appear parallel in an ultrasound image. It is interesting to note that the predicted trend for MT is similar to the observed trend for probe rotations 4-9. This would suggest that if the visualized aponeurosis remained parallel MT behaves similar to the predicted equation. The high reliability of measurement associated with MT, although large compared to the difference noticed in the predicted values, may be sufficient to suggest that an investigator could reliably determine differences in MT based on manual measurement. However, in order to determine the correct probe orientation based on MT, an investigator would need to assume that the muscle behaves similar to the predicted equations and attempt to find the smallest measure of MT. Due to the shape of the observed graph, it is not feasible to declare that the smallest measure of MT is the proper plane of contraction because the smallest measure of MT may not have been visualized in this experiment.

Results from the predicted versus observed comparison on the effect of probe rotation on measures of MAP indicate that there is still reason to believe that probe orientation can affect measures of FL, PA, and MT. The effect of probe orientation can not be entirely predicted with equations or models. Therefore the investigators still

require a more thorough understanding of the effects of probe rotation on the measures of MAP to determine a suitable probe orientation.

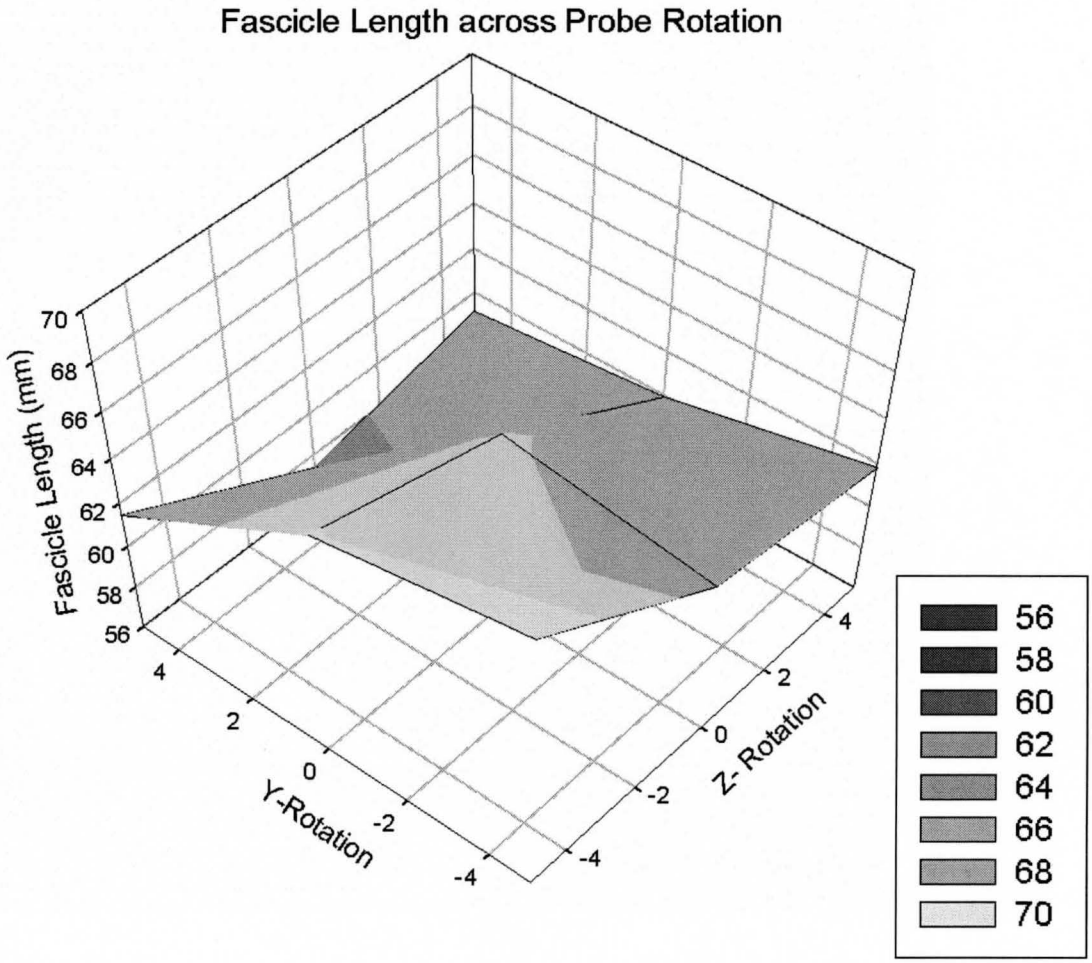

Figure 3-12 The results from a 4(joint angle) X 9 (probe rotation) analysis of variance for measures of FL. The graphs are the Means for Probe Rotation.

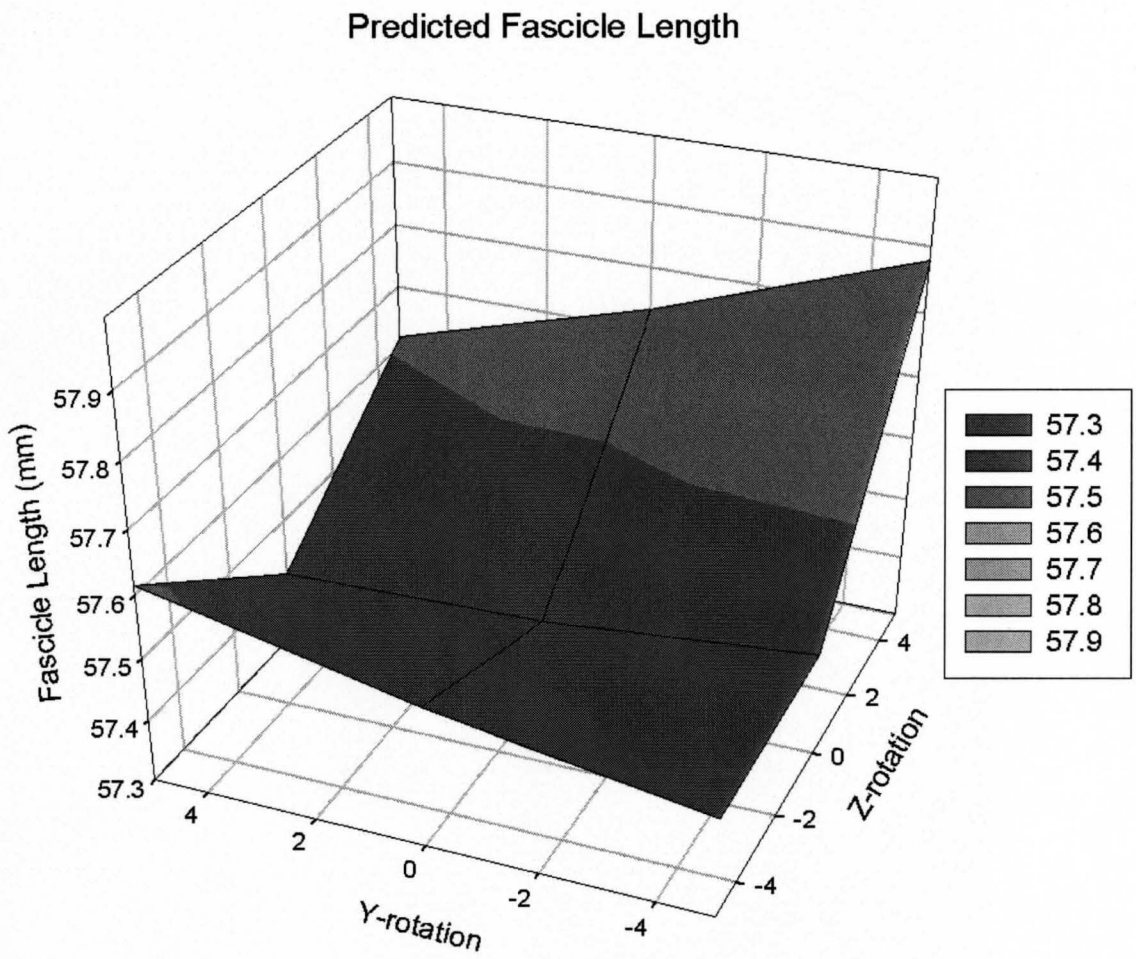

Figure 3-13 The results from a 4(joint angle) X 9 (probe rotation) analysis of variance for measures of fascicle length. The graphs are the Means for Probe Rotation.

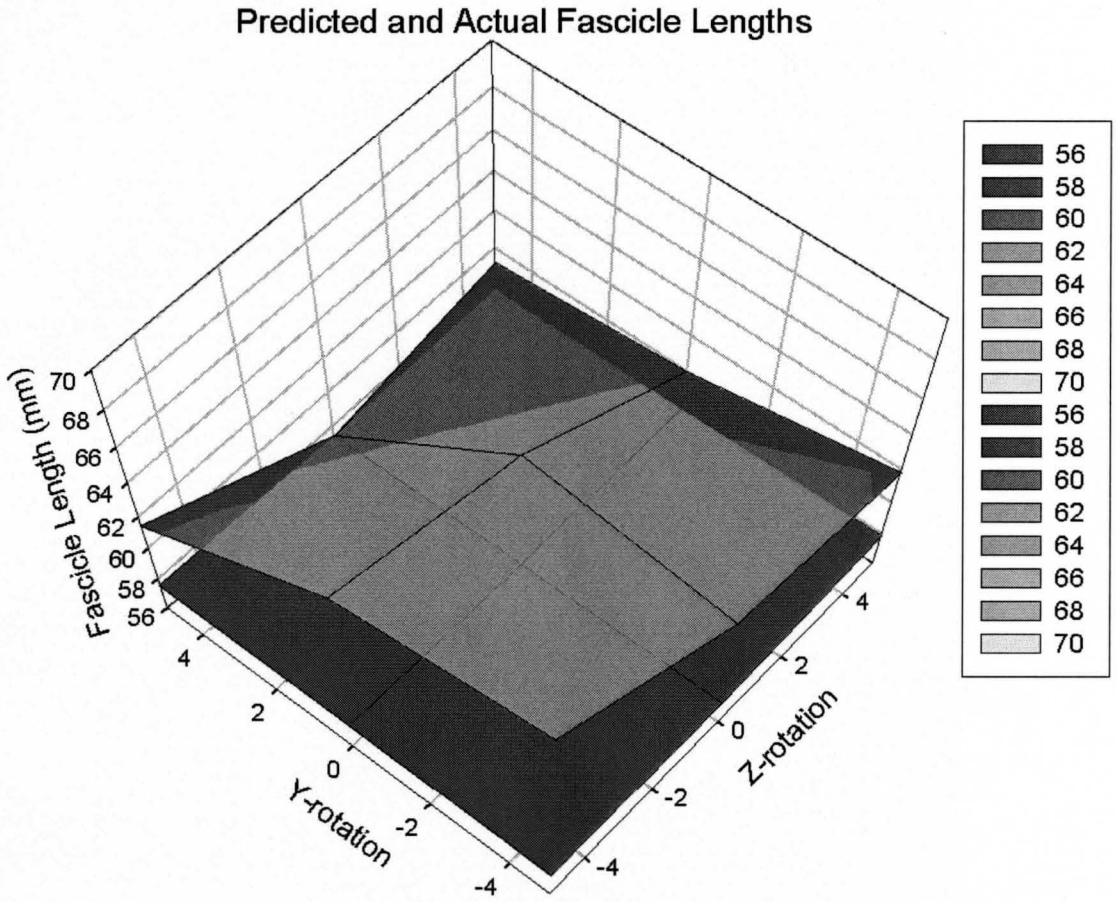

Probe Rotation	Predicted FL (mm)	Observed FL (mm)
1	57.46	67.66
2	57.52	66.15
3	57.62	61.46
4	57.46	62.89
5	57.42	64.19
6	57.41	57.41
7	57.88	61.80
8	57.73	59.93
9	57.62	59.16

Figure 3-14 The results from a 4(joint angle) X 9 (probe rotation) analysis of variance for measures of fascicle length. The graphs are the Means for Probe Rotation.

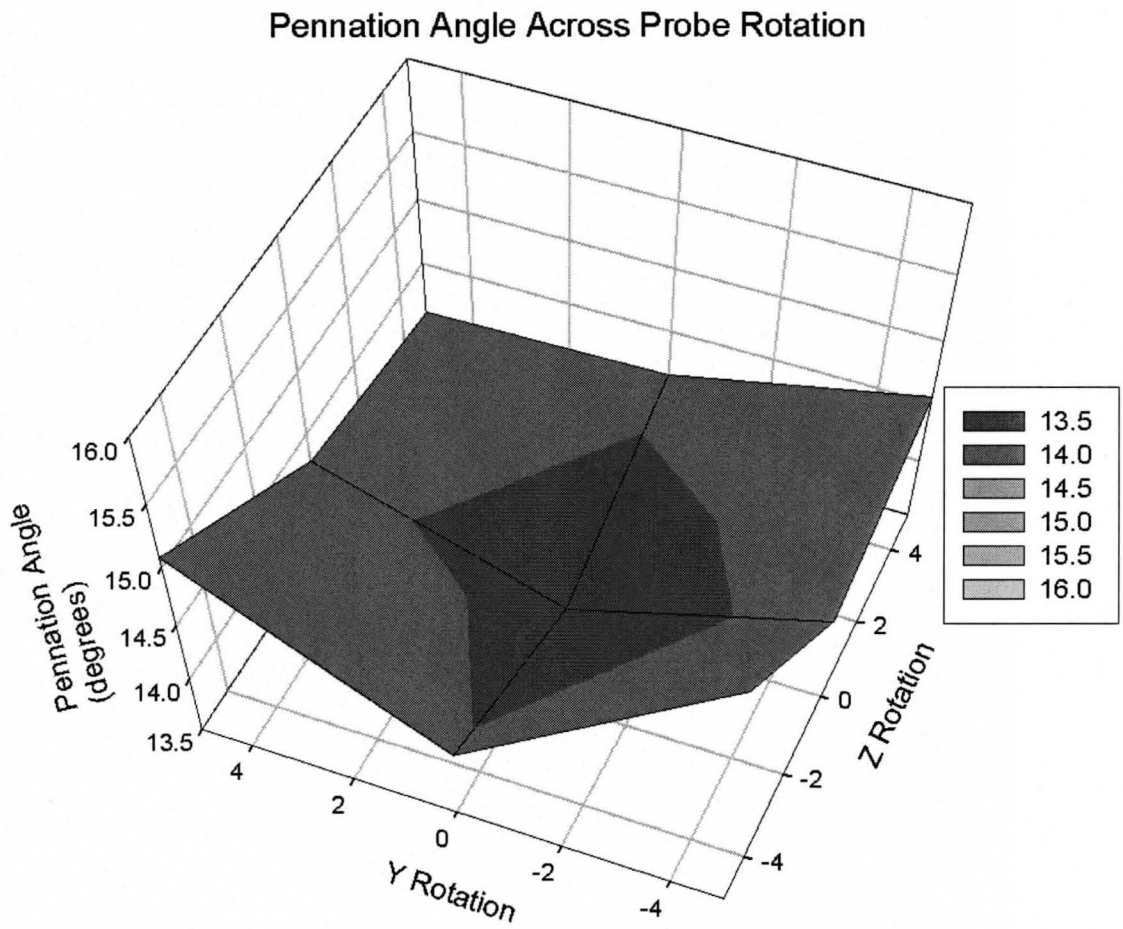

Figure 3-15 The results from a 4(joint angle) X 9 (probe rotation) analysis of variance for measures of Pennation Angle. The graphs are the Means for Probe Rotation.

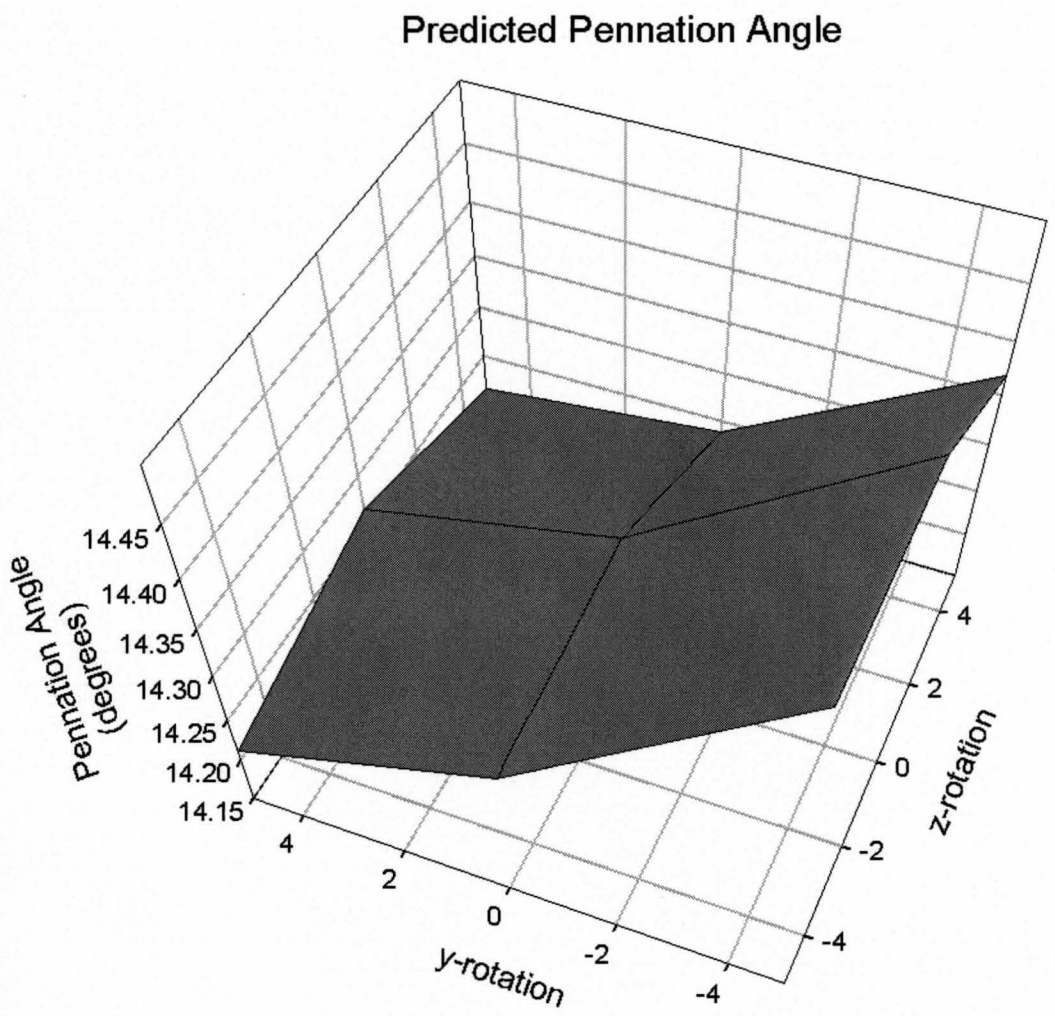

Figure 3-16 The results from a 4(joint angle) X 9 (probe rotation) analysis of variance for measures of pennation angle. The graphs are the Means for Probe Rotation.

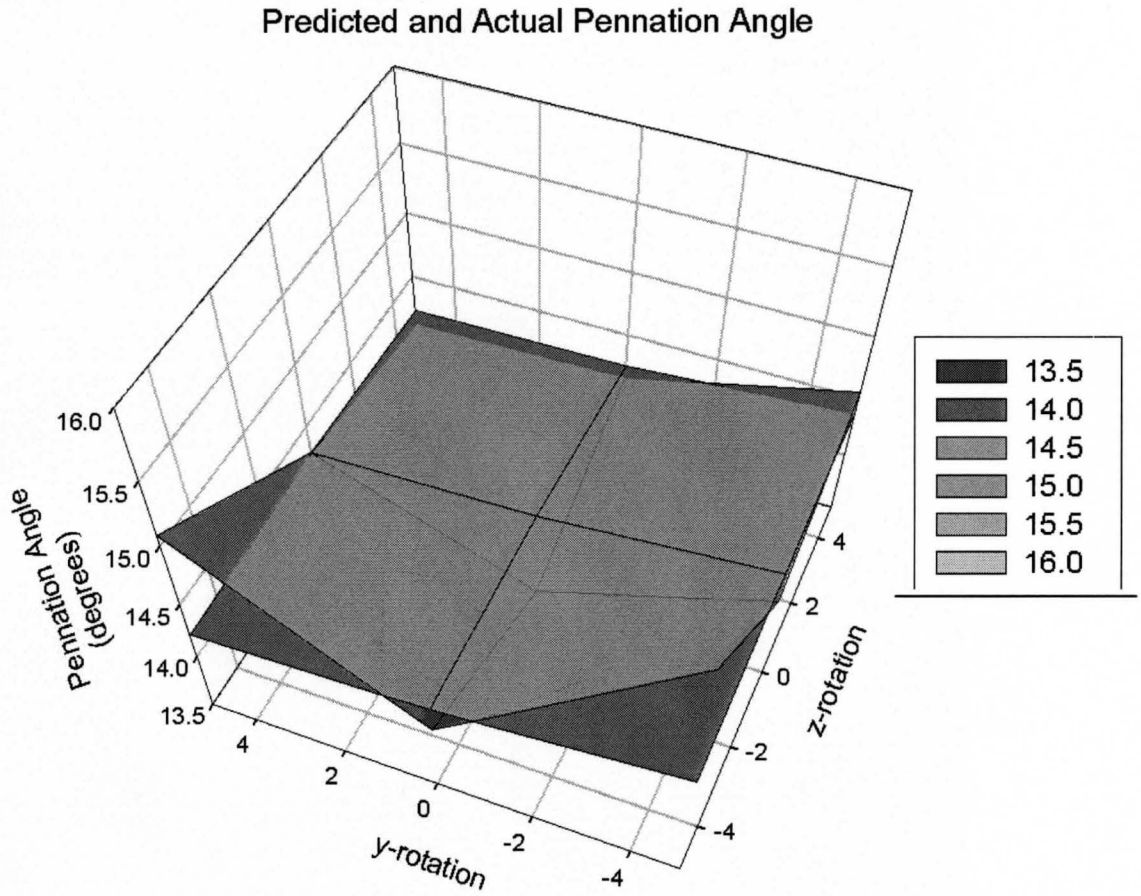

Probe Rotation	Predicted PA (degrees)	Observed PA (degrees)
1	14.48	15.48
2	14.29	14.08
3	14.22	15.08
4	14.48	14.22
5	14.32	13.60
6	14.27	14.27
7	14.37	14.55
8	14.24	14.14
9	14.22	14.10

Figure 3-17 The results from a 4(joint angle) X 9 (probe rotation) analysis of variance for measures of pennation angle. The graphs are the Means for Probe Rotation.

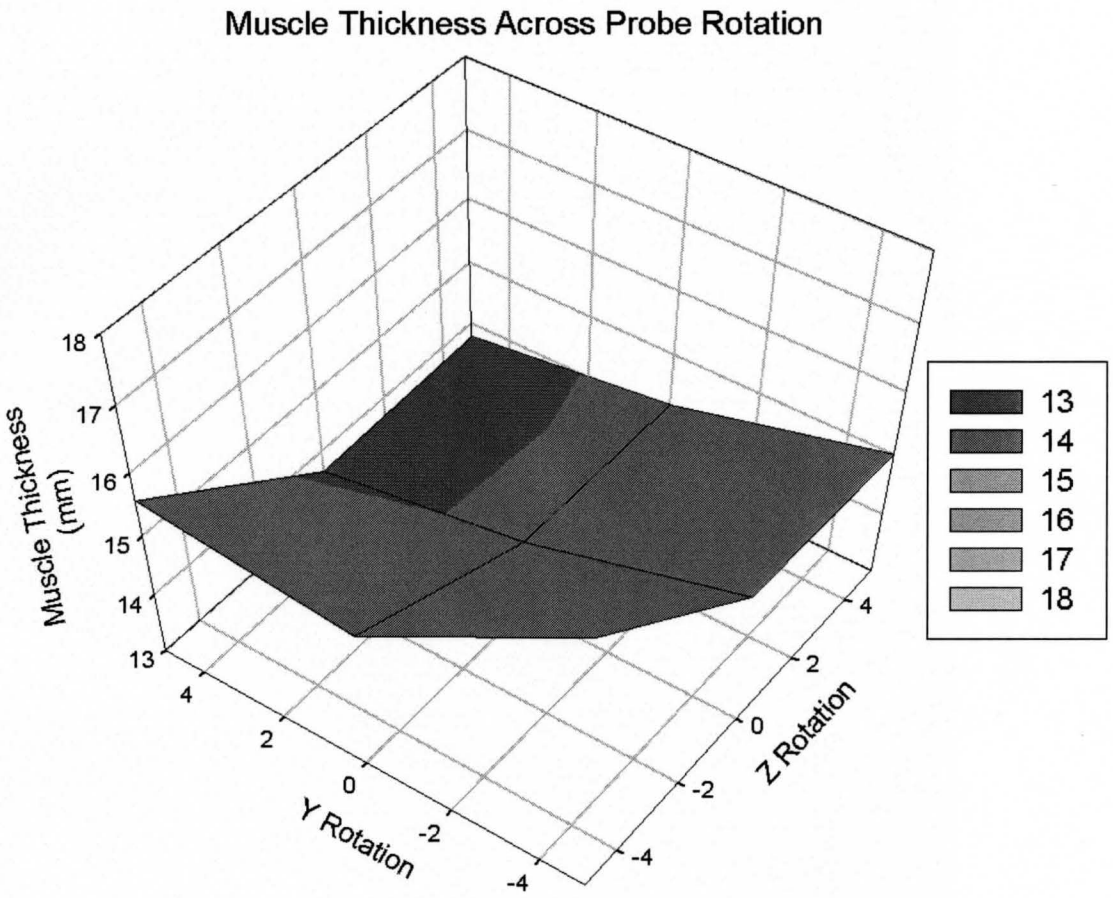

Figure 3-18 The results from a 4(joint angle) X 9 (probe rotation) analysis of variance for measures of Muscle Thickness. The graphs are the Means for Probe Rotation.

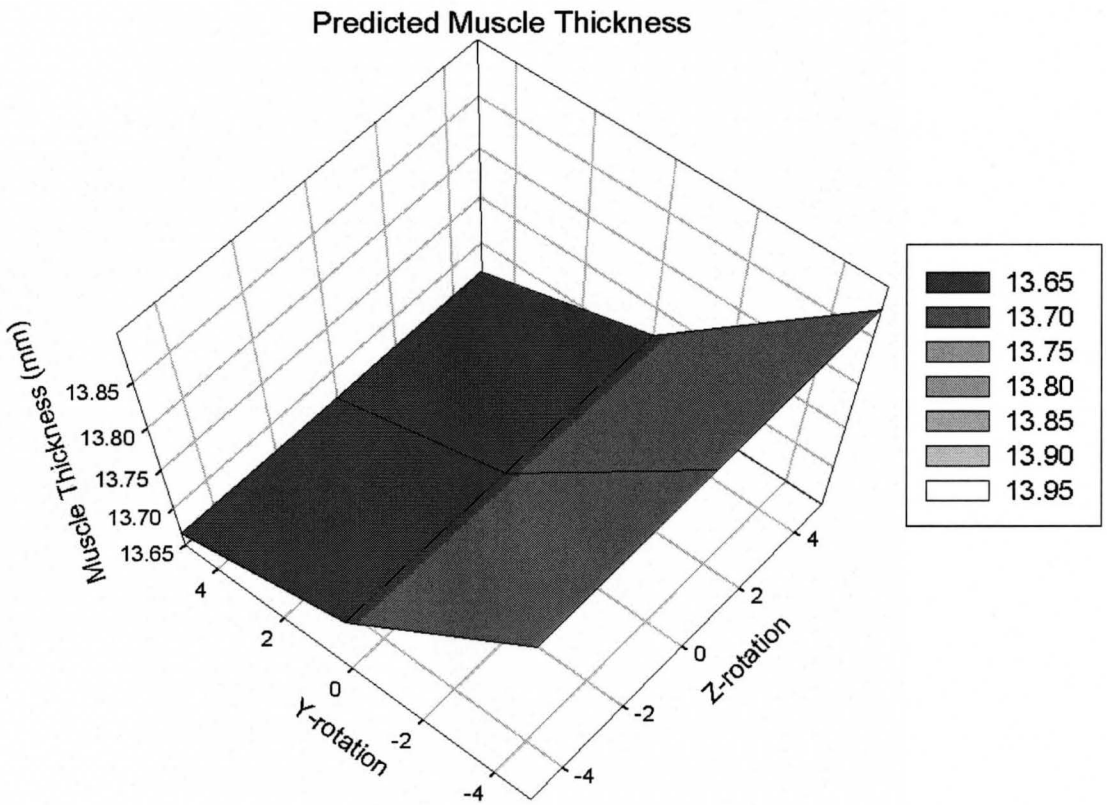

Figure 3-19 The results from a 4(joint angle) X 9 (probe rotation) analysis of variance for measures of Muscle Thickness. The graphs are the Means for Probe Rotation.

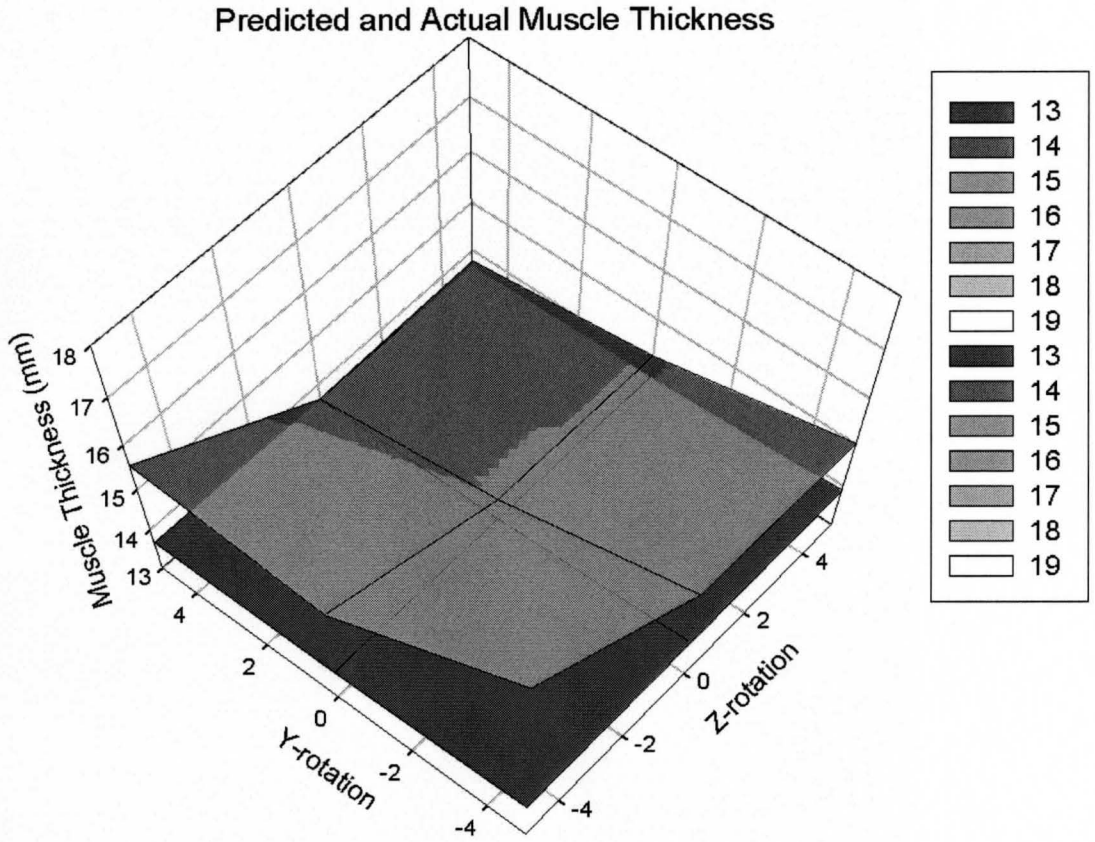

Probe Rotation	Predicted MT (mm)	Observed MT (mm)
1	13.88	17.22
2	13.72	15.25
3	13.67	15.56
4	13.88	15.16
5	13.72	14.21
6	13.67	13.67
7	13.88	14.99
8	13.72	14.18
9	13.67	13.78

Figure 3-20 The results from a 4(joint angle) X 9 (probe rotation) analysis of variance for measures of Muscle Thickness. The graphs are the Means for Probe Rotation.

Future Directions

This section is necessary in order to realize what needs to be done with the information presented in this study. The three major issues that need to be addressed are 1) Improving the reliability of the technique. 2) Applying three dimensional analysis of muscular contraction to validate the use of ultrasound to measure MAP. 3) Initiating a standard or set of guidelines with regards to probe placement and orientation.

The first issue is the improvement of the reliability of the measurement technique. This could be done several ways

i) By increasing the resolution of the images obtained and testing different image filters.

ii) By using ultrasound probes with higher frequencies to increase the spatial resolution.

iii) By creating new methods of determining FL and PA.

iv) By developing automated computer programs to analyze MAP.

The improvement of the measurement technique could allow researchers to determine the exact effect of probe orientation and placement on the measure of MAP.

The second issue is the continuation of the three dimensional analysis of MAP initiated by Kawakami et al. (2000) to determine the structure and movement of fascicles. This type of analysis could further validate the tool of ultrasonography. Through the use of MRI or three-dimensional ultrasound the structure and movement of an individual

fascicle could provide insight into the plane of contraction and plane of visualization dilemma.

The third issue is the need for a standard method or set of guidelines with regards to probe placement and orientation. The movement of a three-dimensional object in a two dimensional window may not be entirely true to life. The tool of ultrasonography to measure MAP has required a thorough understanding of many articles and the ability to understand complex structural relationships. It is extremely important to ensure that a method of measurement is without error or as consistent as possible so that the results from the field may be compared. Without this certainty it is veritably impossible to use this measure to theorize mechanisms for muscular behaviour.

Summary and Conclusion:

An experiment was performed to determine the effect of ultrasound probe orientation on the measurement of MAP. Nine slow dorsi-flexion contractions of the tibialis anterior muscle from nine subjects were compared at four joint angles for measures of torque, EMG, FL, PA and MT.

Results indicate that probe orientation affects measures of FL and MT but not PA.

A reliability study was performed and concluded that MT is a highly reliable measure while PA and FL are not.

Equations were developed to predict the effect of probe orientation on measures of MAP and compared to the experimental observations. These equations were based on observations of investigators conducting muscle architecture parameter research. The predicted values were dissimilar to the observed both in shape and magnitude when

graphed in three dimensions. Therefore, either the predicted equations are not suitable or the measurement technique is not reliable enough to allow the comparison or both.

Muscle thickness could be a necessary and valuable tool to aid researchers in distinguishing the proper probe orientation. MT was found to be a reliable measure which showed the greatest difference for probe orientation. Therefore, with more research MT may be considered an appropriate measure to determine the proper orientation for visualization of MAP with BMU.

Guidelines for the determination of the proper ultrasound probe placement and orientation for tibialis anterior.

For the use of BMU on the measure of MAP on the human tibialis anterior I would suggest these guidelines. Hopefully, these guidelines can produce discussion and comparison of results with the eventual approval of an agreed upon method that all investigators using the tool of BMU to study MAP will facilitate and improve.
The first two instructions are regarding probe placement.

1) Place the probe along the median longitudinal axis of the tibialis anterior muscle which is defined as a straight line drawn between origin and insertion of the muscle, this line is also parallel to the palpable edge of the tibia (Narici et al., 1996; Hodges et al., 2003).

2) Place the probe perpendicular to the dermal surface along the mid-sagittal plane of the TA muscle at the site corresponding to the thickest portion of the muscle (Reeves et al., 2003; Hodges et al., 2003).

The next three instructions require an understanding of the potential effect of probe orientation on the measures of MAP.

3) Rotate the probe in the transverse plane until you have visualized optimally the muscle fascicles and the intramuscular tendon that runs down the centre of the muscle (Hodges et al., 2003).
4) Rotate the probe in the transverse plane until you have found an image where the superficial and deep aponeuroses remain parallel and a fascicle is clearly visualized throughout the movement you wish to perform. This may be achieved by orienting the probe slightly diagonally to the sagittal plane where the probe is oriented perpendicular to the dermal surface (Kawakami et al., 2000)
5) If the superficial and deep aponeuroses are not visualized parallel then rotate the probe in the frontal plane until they are visualized as parallel. This may be further improved by rotating the probe slightly diagonally to the longitudinal axis of the muscle through a rotation in the frontal plane (Reeves et al., 2003; Hodges et al., 2003).

These guidelines have combined the observations of different researchers using this tool and hopefully these guidelines will improve with further research.

References

Aagaard, P., Anderson, J.L., Dyhre-Poulsen, P., Leffers, A.M., Wagner, A., Magnusson, S.P., Halkjaer-Kristensen, J., and E.B. Simonsen. 2001 A mechanism for increased contractile strength of human pennate muscle in response to strength training: changes in muscle architecture. *Journal of Physiology* 534.2: 613-623

Delp, S.L, Suranarayanan, S., Murray, W.M., Uhlir, J., and R.J. Triolo 2001 Architecture of the rectus abdominis, quadratus lumborum, and erector spinae. *Journal of Biomechancis* 34:371-375

Dowling, J.J., 1997 The use of electromyography for the noninvasive prediction of muscle forces; current issues. *Sports Med* 24(2):82-96

Fenn, W.O., 1923 A quantitative comparison between the energy liberated and the work performed by the isolated sartorius muscle of the frog. *Journal of Physiology* 58:175-203

Fenn, W.O., and B.S. Marsh. 1935 Muscular force at different speeds of shortening. *Journal of Physiology* 85:277-297

Fish, P., 1990 *Physics and instrumentation of diagnostic medical ultrasound.* West Sussex: John Wiley & Sons Ltd.

Fukunaga, T., Ichinose,Y., Ito,M.,Kawakami,Y., and S. Fukashiro. 1997 Determination of fascicle length and pennation in a contracting human muscle in vivo. *Journal of Applied Physiology* 82:354-358

Gans, C., and F. De Vree. 1987 Functional basis of fiber length and angulation in muscle. *Journal of Morphology* 192:63-85

Gordon, A.M., Huxley, A.F.,and F.J. Julian. 1964 The length-tension diagram of single vertebrate striated muscle fibres. *Proceedings of the Physiological Society – Royal College of Surgeons Meeting - Journal of Physiology* 171:28-31

Hawkins, D., 2000 A non-invasive approach for studying human muscle-tendon units In vivo. In *Skeletal muscle mechanics: From mechanisms to function..* (ed) Herzog, W., pp.305-326. Toronto: John Wiley & Sons Ltd.

Herbert, R. D., and S.C. Gandevia. 1995 Changes in pennation with joint angle and muscle torque: in vivo measurements in human brachialis muscle. *Journal of Physiology* 484:523–532

Herbert RD, Moseley AM, Butler JE, and S.C. Gandevia. 2002 Change in length of relaxed muscle fascicles and tendons with knee and ankle movement in humans. *Journal of Physiology* 539:637-645

Hill, A. V., 1938 The heat of shortening and the dynamic constants of muscle. *Proc. R. Soc. Lond. B* 126:136-195

Hill, A. V., 1948 The heat of activation and the heat of shortening in a muscle twitch. *Proc. Roy. Soc. Lond. B* 136:195-211

Hill, A.V., 1950 The series elastic component of muscle. *Proc. Roy. Soc. Lond. B* 137: 273-280

Hill, A.V., 1951 The mechanics of voluntary muscle. *The Lancet* 24:947-951

Hill, A.V., 1970 *First and Last Experiments in Muscle Mechanics*. Cambridge: Cambridge University Press.

Hodges, P.W., Pengel, L.H.M., Herbert, R.D., and S.C. Gandevia. 2003 Measurement of muscle contraction with ultrasound imaging. *Muscle & Nerve* 27:682-692

Huijing, P., 1999 Muscle as a collagen fibre reinforced composite: a review of force transmission in muscle and whole limb. *Journal of Biomechanics 32*:329-345

Huxley, A. F.,1957 Muscle structure and theories of contraction. *Prog. Biophys. Biophys.Chem* 7:255-318

Huxley, A. F., and R. Niedergerke.1954 Interference microscopy of living muscle fibers. *Nature* 173:971-973

Huxley, H. E., and J. Hanson. 1954 Changes in cross-striations of muscle during contraction and stretch and their structural interpretation. *Nature* 173:973-976

Huxley, A.F., 2000 Cross bridge action: present views, prospects, and unknowns. In *Skeletal muscle mechanics: From mechanisms to function.* (ed) Herzog, W., pp.7-31. Toronto: John Wiley & Sons Ltd.

Kawakami, Y., Abe, T., and T. Fukunaga. 1993 Muscle-fiber pennation angles are greater in hypertrophied than in normal muscles. *Journal of Applied Physiology* 74(6):2740-2744

Kawakami, Y., Abe, T., Kuno, S., and T. Fukunaga. 1995 Training induced changes in muscle architecture and specific tension. *European Journal of Applied Physiology* 72:37-43

Kawakami, Y., Ichinose, Y., Kubo, K., Ito, M., and T. Fukunaga. 2000 Architecture of contracting human muscles and its functional significance. *J. Appl. Biomech.* 16: 88-97

Kawakami, Y., Muraoka, T.,Ito, S., Kanehisa, H., and T. Fukunaga. 2002 In vivo muscle fibre behaviour during counter-movement exercise in humans reveals a significant role for tendon elasticity. *Journal of Physiology* 540.2: 635-646

Kaya. M., Carvalho. W., Leonard. T., and W. Herzog. 2002 Estimation of cat medial gastrocnemius fascicle lengths during dynamic contractions. *J Biomech.* 35:893-902

Kubo, K., Kanehisa, H., Kawakami, Y., and T. Fukunaga. 2001 Influences of repetitive muscle contractions with different modes on tendon elasticity in vivo. *J Appl Physiol* 91: 277-282

Lieber, R.L., 1999 Skeletal Muscle is a Biological Example of a Linear Electro-Active Actuator. *Proceeding of SPIE's 6th Annual International Symposium on Smart Structures and Materials, San Diego, CA. Paper No. 3669-03.*

Lieber, R.L., 1992 *Skeletal Muscle Structure and Function - Implications for Rehabilitation and Sports Medicine.* Baltimore: Williams & Wilkins.

Maganaris, C. N. & Baltzopoulos, V., and A.J. Sargeant. 1998 In vivo measurements of the triceps surae complex architecture in man: implications for muscle function. *Journal of Physiology* 93:2089-2094

Maganaris, C. N., and V. Baltzopoulos. 1999 Predictability of in vivo changes in pennation angle of human tibialis anterior muscle from rest to maximum isometric dorsiflexion. *Eur J. Appl. Physiol.* 79:294-297

Maganaris, C. N. & Baltzopoulos, V., and A.J. Sargeant. 2002 Repeated contraction alter the geometry of human skeletal muscle. *J. Appl Physiol.* 93: 2089-2094

McComas, A.J. 1996 *Skeletal Muscle; Form and Function.* Illinois:Human Kinetics.

Narici, M. V. T., Binzoni, T., Hiltbrand, E., Fasel, J., Terrier, F., and P. Cerretelli. 1996 In vivo human gastrocnemius architecture with changing joint angle at rest and during graded isometric contraction. *Journal of Physiology* 496:287–297

Nigg, B.M., and W. Herzog. 1999 *Biomechanics of the musculo-skeletal system: second edition.* Toronto:John Wiley & Sons Ltd.

Ramsey, R. W., and S.F. Street. 1940 The isometric length-tension diagram of isolated skeletal muscle fibers of the frog. *J. Cell. Comp. Physiol.* 15:11-34

Reeves., N.D. and M.V. Narici. 2003 Behavior of human muscle fascicles during shortening and lengthening contractions in vivo. *J. Appl. Physiol.* 95(3):1090-1096

Scott, S.H. Engstrom, C. M., and G.E. Loeb. 1993 Morphometry of human thigh muscles . Determination of fascicle architecture by magnetic resonance imaging. *Journal of Anatomy* 182:249-257

Street, S.F., and R.W. Ramsey. 1965 Sarcolemma transmitter of active tension in frog skeletal muscle. *Science* 149:1379-1380

T. L. Wickiewicz, R. R. Roy, P. L. Powell, J. J. Perrine, and V. R. Edgerton. 1984 Muscle architecture and force-velocity relationships in humans. *J Appl Physiol* 57: 435-443

Zagzebski, J. A., 1986 *Introduction to Vascular Ultrasonography : Second Edition.* (ed) William J. Zwiebel. Grune & Stratton, Inc.

Appendix: A

Repeated Measures Analysis of Variance (Tibialis EMG) Effective hypothesis decomposition					
	SS	df	MS	F	p
JA	242743	3	80914	21.50074	0.000001
PR	8614	8	1077	1.19852	0.314175
JA*PR	17935	24	747	1.29116	0.173888

Repeated Measures Analysis of Variance (PA) Effective hypothesis decomposition					
	SS	df	MS	F	p
JA	1055.54	3	351.85	148.4867	0.000000
PR	93.62	8	11.70	1.3537	0.234084
JA*PR	12.38	24	0.52	0.5741	0.945391

Repeated Measures Analysis of Variance (MT) Effective hypothesis decomposition					
	SS	df	MS	F	p
JA	0.03	3	0.01	0.0103	0.998527
PR	352.86	8	44.11	5.7953	0.000015
JA*PR	3.13	24	0.13	1.4445	0.091050

Repeated Measures Analysis of Variance (FL) Effective hypothesis decomposition					
	SS	df	MS	F	p
JA	21057	3	7019	79.7461	0.000000
PR	3160	8	395	2.6906	0.012895
JA*PR	362	24	15	0.5889	0.936967

Repeated Measures Analysis of Variance (Torque) Effective hypothesis decomposition					
	SS	df	MS	F	p
JA	377.0	3	125.7	8.6252	0.000463
PR	13.0	8	1.6	1.3716	0.226030
JA*PR	59.1	24	2.5	0.7698	0.771327